Finite-temperature correlations for the $U_q(sl(2|1))$-invariant generalized Hubbard model

2001 J. Phys. A: Math. Gen. 34 8015

(http://iopscience.iop.org/0305-4470/34/39/307)

INSTITUTE OF PHYSICS PUBLISHING JOURNAL OF PHYSICS A: MATHEMATICAL AND GENERAL

J. Phys. A: Math. Gen. **34** (2001) 8015–8055 PII: S0305-4470(01)25188-9

Finite-temperature correlations for the $U_q(\mathfrak{sl}(2|1))$-invariant generalized Hubbard model

Kazumitsu Sakai and Andreas Klümper

Theoretische Physik I, Universität Dortmund, Otto-Hahn-Str. 4, D-44221 Dortmund, Germany

E-mail: sakai@printfix.physik.uni-dortmund.de, kluemper@printfix.physik.uni-dortmund.de

Received 24 May 2001
Published 21 September 2001
Online at stacks.iop.org/JPhysA/34/8015

Abstract

We study an integrable model of one-dimensional strongly correlated electrons at finite temperature by explicit calculation of the correlation lengths of various correlation functions. The model is invariant with respect to the quantum superalgebra $U_q(\mathfrak{sl}(2|1))$ and characterized by the Hubbard interaction, correlated hopping and pair-hopping terms. Using the integrability, the graded quantum transfer matrix is constructed. From the analyticity of its eigenvalues, a closed set of nonlinear integral equations is derived which describe the thermodynamical quantities and the finite-temperature correlations. The results show a crossover from a regime with dominating density–density correlations to a regime with dominating superconducting pair correlations. Analytical calculations in the low-temperature limit are also discussed.

PACS numbers: 75.10.Jm, 05.50+q

Dedicated to E Müller-Hartmann on the occasion of his 60th birthday.

1. Introduction

In recent decades, integrable models in one-dimensional strongly correlated electron systems have attracted considerable attention in relation to high-T_c superconductivity. In general, integrable models are solvable by means of the Bethe ansatz. The critical exponents of the correlation functions depend only on the R-matrix of the underlying infinite-dimensional symmetry and the geometry of the Fermi sea of the ground state (see the book [1] and references therein). This important fact shows that all integrable models with a given R-matrix exhibit the same universal critical behaviour.

On the other hand $(1 + 1)$-dimensional critical phenomena are connected with conformal field theory (CFT) [2]. The central charge and conformal dimensions are calculated by the scaling behaviour of the ground state and the low-lying excitations [3]. The conformal dimensions determine the long-distance asymptotics of all correlation functions of any local operators. For integrable models, one obtains the conformal dimensions by use of the Bethe

ansatz in terms of the so-called dressed charge function satisfying a linear integral equation. Thus the Bethe ansatz together with CFT provide a powerful tool to study the correlation functions especially at the critical point $T = 0$ [4, 5].

For finite temperatures, however, one encounters technical difficulties. Despite the fact that the models are still solvable even off criticality, the above powerful methods lose effect due to the collapse of conformal invariance. Qualitatively, we see that the long-distance behaviour of the correlation functions show exponential decay and calculate the low temperature asymptotics by extension of the conformal mapping (see, for example, [1]). However, we need another approach for the *quantitative* understanding of the correlation functions at finite temperatures.

As a totally different approach, the quantum transfer matrix (QTM) has been proposed recently to overcome such difficulties [6–16]. Originally the QTM method was developed as an alternative method to traditional thermodynamical studies [17–19]. Utilizing the Trotter mapping, one deals with a two-dimensional classical system instead of the original one-dimensional quantum system. Using the underlying integrability, one constructs a family of *commuting* QTMs [15, 16]. The commuting QTMs are diagonalized by means of the Bethe ansatz. Thermodynamical quantities are expressed in terms of the sole largest eigenvalue. Also, this procedure has remarkable advantages for the study of correlation functions, which is the main topic of our paper. Explicitly, the correlation lengths can be calculated by taking ratios of the largest eigenvalue and the sub-leading ones [8, 13, 14, 16, 20–23].

In this paper we study a strongly correlated electron system using the approach sketched above. As a result, we evaluate the six crucial correlation lengths for arbitrary particle densities and finite temperatures: (i) the longitudinal and (ii) transversal spin–spin correlations, (iii) the density–density correlations, (iv) the one-particle Green function, (v) the singlet and (vi) triplet superconducting pair correlations. These are the first quantitative calculations for correlation functions of strongly correlated electron systems off criticality.

The Hamiltonian of the model [24] on a periodic lattice of size L is defined by

$$\mathcal{H} = -\sum_{j=1}^{L}\sum_{\sigma=\uparrow,\downarrow}(c^{\dagger}_{j,\sigma}c_{j+1,\sigma} + c^{\dagger}_{j+1,\sigma}c_{j,\sigma})\exp\left(-\tfrac{1}{2}(\eta-\sigma\gamma)n_{j,\sigma} - \tfrac{1}{2}(\eta+\sigma\gamma)n_{j+1,-\sigma}\right)$$
$$+U\sum_{j=1}^{L}n_{j,\uparrow}n_{j,\downarrow} + t_p\sum_{j=1}^{L}(c^{\dagger}_{j+1,\uparrow}c^{\dagger}_{j+1,\downarrow}c_{j,\uparrow}c_{j,\downarrow} + c^{\dagger}_{j,\uparrow}c^{\dagger}_{j,\downarrow}c_{j+1,\uparrow}c_{j+1,\downarrow}) \tag{1.1}$$

where $c^{\dagger}_{j,\sigma}$ ($c_{j,\sigma}$) denotes the fermion creation (annihilation) operator at the jth site satisfying the canonical aniticommutation relations

$$\{c^{\dagger}_{j,\sigma}, c^{\dagger}_{k,\tau}\} = \{c_{j,\sigma}, c_{k,\tau}\} = 0 \qquad \{c^{\dagger}_{j,\sigma}, c_{k,\tau}\} = \delta_{jk}\delta_{\sigma\tau} \tag{1.2}$$

and $n_{j,\sigma}$ is the number operator, i.e. $n_{j,\sigma} = c^{\dagger}_{j,\sigma}c_{j,\sigma}$. The ground state properties and the long-distance behaviour of the correlation functions have been studied in [24] by the Bethe ansatz and CFT. Due to the massive spin excitations ($\gamma \neq 0$), the ground state properties are described by a one-component Tomonaga–Luttinger liquid (Luther–Emery liquid). For this system the one-particle Green function decays exponentially fast, the density–density and certain pair correlations are quasi-longranged with algebraic decay. As the model is one-dimensional it does not exhibit off-diagonal long-range order. However, the crossover behaviour from dominant density–density correlations to dominant (singlet) pair correlations driven by the density of particles manifests superconducting properties. More quantitatively, on the basis of scaling arguments and RG concepts we would expect that higher-dimensional interactions such as interchain couplings are relevant and may lead to true condensation of Cooper pairs.

The model is related to a trigonometric R-matrix which is a solution to the graded YBE [25] associated with the four-dimensional irreducible representation of the quantum superalgebra $U_q(\mathfrak{sl}(2|1))$ [26] (see also [27] for the rational case $\gamma = 0$). The diagonalization of the Hamiltonian for general η and γ was done in [24] and the diagonalization of the associated row-to-row transfer matrix was done for the rational case $\gamma = 0$ in [28,29,36]. The thermodynamics have been investigated by the traditional thermodynamic Bethe ansatz based on the string hypothesis in [30] and the present approach in [31].

The asymptotic behaviour of correlation functions of this model has been studied so far only for the ground state where a crossover was established from a normal to a 'superconducting' regime driven by the particle density. Here we want to extend this study to finite temperatures where we are especially interested in the extension of the 'superconducting regime' in the density–temperature phase diagram. For this purpose we define the QTM acting on a $\mathbb{Z}_2$-graded vector space. As a consequence, the genuine fermionic statistics are built into the QTM algebraically through the Grassmann parity $p[j]$ (see equation (2.26)). Regarding the thermodynamical quantities, one might content oneself with the corresponding null Grassmann parity model, because the fermionic statistics do not affect the thermodynamical quantities directly. (We obtain the null-parity model satisfying the ordinary Yang–Baxter equation by multiplying the original graded R-matrix by suitable minus signs.) However, one must be careful to keep track of the fermionic statistics when considering the physical quantities changing the particle number. As the auxiliary and quantum space are the same graded vector space, we easily obtain the eigenvalues of the QTM by using the results from the algebraic Bethe ansatz for the row-to-row transfer matrix. The resultant eigenvalues can be expressed in the dressed vacuum form (DVF) via the Bethe ansatz equation (BAE). The difference between the DVF of the QTM and the one of the row-to-row transfer matrix consists only of their vacuum parts. Hence, in the actual calculation to the DVF, one utilizes the methods developed in the finite-size correction problem [32]. In consequence, all information of the BAE is contained in three nonlinear integral equations (NLIEs), which are valid for a system with any Trotter number N. In this approach, the limit $N \to \infty$ can be taken *analytically*. This finite set of NLIEs allows for highly accurate numerical calculations of physical quantities such as the above-mentioned correlation lengths. In particular, we observe temperature-dependent crossover phenomena between regimes dominated by density–density or (singlet) superconducting pair correlations, respectively.

At low temperatures, the three NLIEs are reduced to only one *linear* integral equation, which reflects the one-component Tomonaga–Luttinger (Luther–Emery) liquid properties. This linear equation is evaluated analytically and reproduces the predictions from CFT. The formulations in this paper are applicable to various kinds of strongly correlated electron systems which have superalgebra invariance: for example, the supersymmetric extended Hubbard model ($\mathfrak{sl}(2|2)$-invariance) [33, 34].

The layout of this paper is as follows. In section 2 we define the commuting QTM constructed by the graded R-matrix. The QTM is diagonalized by the algebraic Bethe ansatz in analogy to the ordinary row-to-row transfer matrix. In section 3 we study the eigenvalues by introducing certain auxiliary functions. Investigating their analyticity, we determine the NLIE for the largest and sub-leading eigenvalues. We obtain six sets of NLIEs characterizing the above-mentioned correlations. The numerical results for these NLIEs are discussed. Section 4 is devoted to the analytical calculation of the low-temperature asymptotics of the correlations characterized by gapless excitations. Section 5 contains our conclusions. Details of technical calculations are summarized in various appendices.

2. The graded quantum transfer matrix

The model (1.1) is solvable under the conditions

$$t_p = \frac{U}{2} = \frac{\mathrm{sh}\gamma}{\mathrm{sh}\alpha\gamma} \qquad \exp(-\eta) = \frac{\mathrm{sh}(\alpha+1)\gamma}{\mathrm{sh}\alpha\gamma}. \tag{2.1}$$

Here the physical region of the two parameters α and γ is restricted to $\gamma \geqslant 0$ and $\alpha > 0$ (repulsive) or $\alpha < -1$ (attractive). (This does not include the pure Hubbard model which corresponds to $\eta = \gamma = t_p = 0$ and $U \neq 0$ violating (2.1). Note however, that a unified treatment of the $U_q(\mathfrak{sl}(2|1))$-invariant generalized Hubbard model and the standard Hubbard model might be possible on the basis of the work in [35].)

Several prominent models are comprised as special cases: the supersymmetric $t-J$ model ($\gamma = 0, \alpha \to 0$), the pure correlated-hopping model ($|\alpha| \to \infty$) and a model of hard-core particles of three species (doubly occupied site, single electron with spin pointing either up or down) ($\alpha \to -1$). For any finite γ the spinon excitations have a mass gap and so do single-particle excitations. The pair excitations (singlet) and the particle–hole type excitations are massless. The former excitations become gapless for the repulsive case ($\alpha > 0$) in the rational limit $\gamma = 0$. Consequently, for $\gamma > 0$ the one-particle Green function shows exponential decay and hence the momentum distribution function has no singularity at the Fermi point.

The classical counterpart of this model is given by a trigonometric R-matrix which is associated with the one parameter family of the four-dimensional irreducible representation of the quantum superalgebra $U_q(\mathfrak{sl}(2|1))$ [26] (see also [27] for the rational case $\gamma = 0$). Choosing the following basis:

$$|1\rangle \equiv |\uparrow\downarrow\rangle = c_\downarrow^\dagger c_\uparrow^\dagger|0\rangle \qquad |2\rangle \equiv |\downarrow\rangle = c_\downarrow^\dagger|0\rangle \qquad |3\rangle \equiv |\uparrow\rangle = c_\uparrow^\dagger|0\rangle \qquad |4\rangle \equiv |0\rangle \tag{2.2}$$

with grading $|1\rangle, |4\rangle$ even (bosonic) and $|2\rangle, |3\rangle$ odd (fermionic), one determines the following 36 non-zero matrix elements:

$$\begin{aligned}
&R_{11}^{11}(v) = \frac{[2\alpha - v]}{[2\alpha + v]} \qquad R_{22}^{22}(v) = R_{33}^{33}(v) = -1 \qquad R_{44}^{44}(v) = \frac{[2\alpha + 2 + v]}{[2\alpha + 2 - v]} \\
&R_{12}^{12}(v) = R_{13}^{13}(v) = R_{21}^{21}(v) = R_{31}^{31}(v) = -\frac{[v]}{[2\alpha + v]} \\
&R_{24}^{24}(v) = R_{34}^{34}(v) = R_{42}^{42}(v) = R_{43}^{43}(v) = \frac{[v]}{[2\alpha + 2 - v]} \\
&R_{14}^{14}(v) = R_{41}^{41}(v) = \frac{[v][v-2]}{[2\alpha + v][2\alpha + 2 - v]} \qquad R_{23}^{23}(v) = R_{32}^{32}(v) = \frac{[v]^2}{[2\alpha + v][2\alpha + 2 - v]} \\
&R_{12}^{21}(v) = R_{13}^{31}(v) = \frac{\mathrm{e}^{-\gamma v/2}[2\alpha]}{[2\alpha + v]} \qquad R_{21}^{12}(v) = R_{31}^{13}(v) = \frac{\mathrm{e}^{\gamma v/2}[2\alpha]}{[2\alpha + v]} \\
&R_{14}^{41}(v) = \frac{\mathrm{e}^{-\gamma v}[2\alpha][2\alpha + 2]}{[2\alpha + v][2\alpha + 2 - v]} \qquad R_{41}^{14}(v) = \frac{\mathrm{e}^{\gamma v}[2\alpha][2\alpha + 2]}{[2\alpha + v][2\alpha + 2 - v]} \\
&R_{23}^{32}(v) = \frac{-\mathrm{e}^{\gamma v/2}[2][v] - [2\alpha][2\alpha + 2]}{[2\alpha + v][2\alpha + 2 - v]} \qquad R_{32}^{23}(v) = \frac{-\mathrm{e}^{-\gamma v/2}[2][v] - [2\alpha][2\alpha + 2]}{[2\alpha + v][2\alpha + 2 - v]} \\
&R_{24}^{42}(v) = R_{34}^{43}(v) = \frac{\mathrm{e}^{-\gamma v/2}[2\alpha + 2]}{[2\alpha + 2 - v]} \qquad R_{42}^{24}(v) = R_{43}^{34}(v) = \frac{\mathrm{e}^{\gamma v/2}[2\alpha + 2]}{[2\alpha + 2 - v]} \\
&R_{14}^{23}(v) = -R_{32}^{41}(v) = -\frac{\sqrt{[2\alpha][2\alpha + 2]}\mathrm{e}^{-\gamma(1+v)/2}[v]}{[2\alpha + v][2\alpha + 2 - v]} \\
&R_{14}^{32}(v) = -R_{23}^{41}(v) = \frac{\sqrt{[2\alpha][2\alpha + 2]}\mathrm{e}^{\gamma(1-v)/2}[v]}{[2\alpha + v][2\alpha + 2 - v]}
\end{aligned} \tag{2.3}$$

$$R_{23}^{14}(v) = -R_{41}^{32}(v) = -\frac{\sqrt{[2\alpha][2\alpha+2]}\mathrm{e}^{\gamma(1+v)/2}[v]}{[2\alpha+v][2\alpha+2-v]}$$
$$R_{32}^{14}(v) = -R_{41}^{23}(v) = \frac{\sqrt{[2\alpha][2\alpha+2]}\mathrm{e}^{-\gamma(1-v)/2}[v]}{[2\alpha+v][2\alpha+2-v]}$$

where $R_{\alpha\beta}^{\gamma\delta}(v)$ are defined by

$$R(v)|\alpha\rangle \underset{s}{\otimes} |\beta\rangle = |\gamma\rangle \underset{s}{\otimes} |\delta\rangle R_{\alpha\beta}^{\gamma\delta}(v) \tag{2.4}$$

with $[v] := \mathrm{sh}(\gamma v/2)$ and the graded tensor product satisfies $P|\alpha\rangle \otimes_s |\beta\rangle := (-)^{p[\alpha]p[\beta]}|\beta\rangle \otimes_s |\alpha\rangle$ where P denotes permutation. This R-matrix is known to satisfy the graded Yang–Baxter equation (GYBE) [25]

$$R_{12}(u-v)R_{13}(u)R_{23}(v) = R_{23}(v)R_{13}(u)R_{12}(u-v) \tag{2.5}$$

which explicitly reads in terms of the matrix elements

$$R_{\gamma_1\gamma_2}^{\beta_1\beta_2}(u-v)R_{\alpha_1\gamma_3}^{\gamma_1\beta_3}(u)R_{\alpha_2\alpha_3}^{\gamma_2\gamma_3}(v)(-)^{(p[\alpha_1]+p[\gamma_1])p[\gamma_2]}$$
$$= R_{\gamma_2\gamma_3}^{\beta_2\beta_3}(v)R_{\gamma_1\alpha_3}^{\beta_1\gamma_3}(u)R_{\alpha_1\alpha_2}^{\gamma_1\gamma_2}(u-v)(-)^{(p[\beta_1]+p[\gamma_1])p[\gamma_2]} \tag{2.6}$$

where the Grassmann parity $p[j]$ is defined by $p[1] = p[4] = 0$ (bosonic), $p[2] = p[3] = 1$ (fermionic). In equation (2.6) and later we sum over repeated indices. Note that the parity of the R-matrix is even, i.e.

$$p[R] \equiv p[\alpha] + p[\beta] + p[\gamma] + p[\delta] \equiv 0 \bmod 2. \tag{2.7}$$

To relate model (1.1) to the above classical model, we construct the graded transfer matrix

$$T(v) = \mathrm{Str}_a\{R_{aL}(v)\ldots R_{a2}(v)R_{a1}(v)\}. \tag{2.8}$$

Using the R-matrix parity (2.7), one writes explicitly the transfer matrix by means of the matrix elements (2.4)

$$T_{\alpha_1\alpha_2\ldots\alpha_L}^{\beta_1\beta_2\ldots\beta_L}(v) = (-)^{p[a]+\sum_{j=2}^{L}(p[\alpha_j]+p[\beta_j])\sum_{k=1}^{j-1}p[\beta_k]}R_{\gamma_{L-1}\alpha_L}^{a\ \ \beta_L}(v)\ldots R_{\gamma_1\alpha_2}^{\gamma_2\beta_2}(v)R_{a\ \alpha_1}^{\gamma_1\beta_1}(v). \tag{2.9}$$

Due to the GYBE (2.5), the transfer matrices $T(v)$ commute for different spectral parameters v and v'

$$[T(v), T(v')] = 0. \tag{2.10}$$

Using the fact that the local Hamiltonian $\mathcal{H}_{jj+1}$ can be expressed as the derivative of $R_{jj+1}(v)$

$$\mathcal{H}_{jj+1} = -\frac{2\mathrm{sh}(\alpha+1)\gamma}{\gamma}P_{jj+1}\frac{\mathrm{d}}{\mathrm{d}v}R_{jj+1}(v)\bigg|_{v=0}$$
$$+2\mathrm{ch}(\alpha+1)\gamma - 2(n_{j,\uparrow}+n_{j,\downarrow}+n_{j+1,\uparrow}+n_{j+1,\downarrow})\mathrm{ch}(\alpha+1)\gamma \tag{2.11}$$

we can expand the transfer matrix $T(v)$ with respect to v as

$$T(v) = T(0)\left(1 - \frac{\gamma v}{2\mathrm{sh}(\alpha+1)\gamma}\mathcal{H}' + \mathrm{O}(v^2)\right). \tag{2.12}$$

Here we have introduced the superpermutation operator P_{jj+1} whose matrix elements are

$$[P_{jj+1}]_{\alpha\beta}^{\gamma\delta} = [R_{jj+1}(0)]_{\alpha\beta}^{\gamma\delta} = (-)^{p[\alpha]p[\beta]}\delta_{\alpha\delta}\delta_{\beta\gamma}. \tag{2.13}$$

Note that $\mathcal{H}'$ denotes the Hamiltonian (1.1) with shifted chemical potential and ground state energy

$$\mathcal{H}' = \mathcal{H} - 2L\mathrm{ch}(\alpha+1)\gamma + 2\mathcal{N}_\mathrm{e}\mathrm{ch}(\alpha+1)\gamma \tag{2.14}$$

where $\mathcal{N}_\mathrm{e}$ is the electron number operator.

In order to treat the finite-temperature case, we consider another R-matrix defined by

$$\overline{R}^{\gamma\delta}_{\alpha\beta}(v) = (-)^{p[\beta](p[\alpha]+p[\gamma])} R^{\delta\alpha}_{\beta\gamma}(v). \tag{2.15}$$

This matrix $\overline{R}$ satisfies the following type of GYBE:

$$\overline{R}_{12}(v-u)\overline{R}_{13}(-u)R_{23}(v) = R_{23}(v)\overline{R}_{13}(-u)\overline{R}_{12}(v-u) \tag{2.16}$$

which reads explicitly

$$\begin{aligned}&\overline{R}^{\beta_1\beta_2}_{\gamma_1\gamma_2}(v-u)\overline{R}^{\gamma_1\beta_3}_{\alpha_1\gamma_3}(-u)R^{\gamma_2\gamma_3}_{\alpha_2\alpha_3}(v)(-)^{(p[\alpha_1]+p[\gamma_1])p[\gamma_2]}\\ &\quad = R^{\beta_2\beta_3}_{\gamma_2\gamma_3}(v)\overline{R}^{\beta_1\gamma_3}_{\gamma_1\alpha_3}(-u)\overline{R}^{\gamma_1\gamma_2}_{\alpha_1\alpha_2}(v-u)(-)^{(p[\beta_1]+p[\gamma_1])p[\gamma_2]}.\end{aligned} \tag{2.17}$$

Using this, one constructs the transfer matrix

$$\overline{T}(v) = \mathrm{Str}_a\{\overline{R}_{aL}(v)\dots\overline{R}_{a2}(v)\overline{R}_{a1}(v)\} \tag{2.18}$$

explicitly reading

$$\overline{T}^{\beta_1\beta_2\dots\beta_L}_{\alpha_1\alpha_2\dots\alpha_L}(v) = (-)^{p[a]+\sum_{j=2}^{L}(p[\alpha_j]+p[\beta_j])\sum_{k=1}^{j-1}p[\beta_k]}\overline{R}^{a\ \ \beta_L}_{\gamma_{L-1}\alpha_L}(v)\dots\overline{R}^{\gamma_2\beta_2}_{\gamma_1\alpha_2}(v)\overline{R}^{\gamma_1\beta_1}_{a\ \alpha_1}(v). \tag{2.19}$$

We expand this transfer matrix in the same manner as (2.12),

$$\overline{T}(v) = \overline{T}(0)\left(1 - \frac{\gamma v}{2\mathrm{sh}(\alpha+1)\gamma}\mathcal{H}' + \mathrm{O}(v^2)\right). \tag{2.20}$$

Combining the above relations and using $\overline{T}(0)T(0) = 1$ (note that $T(0)$ and $\overline{T}(0)$ denote the right and left shift operators, respectively), one obtains

$$\overline{T}(u)T(u) = 1 - \frac{\gamma u}{\mathrm{sh}(\alpha+1)\gamma}\mathcal{H}' + \mathrm{O}(v^2). \tag{2.21}$$

From the above equation, it follows that

$$\exp(-\beta\mathcal{H}') = \lim_{N\to\infty}\left[\overline{T}(u_N)T(u_N)\right]^{N/2} \qquad u_N = \frac{2\beta\mathrm{sh}(\alpha+1)\gamma}{N\gamma}. \tag{2.22}$$

Here β is the reciprocal temperature; $\beta = 1/T$ and the height N of the fictitious underlying square lattice is even and referred to as the Trotter number. Hence the free energy f of the original quantum system (1.1) is given by

$$f = -\lim_{L\to\infty}\lim_{N\to\infty}\frac{1}{L\beta}\ln\left(\mathrm{Tr}\left[\overline{T}(u_N)T(u_N)\right]^{N/2}\right) + 2(1-n_\mathrm{e})\mathrm{ch}(\alpha+1)\gamma \tag{2.23}$$

where n_e denotes the particle density of the system. Calculating $\mathrm{Tr}\left[\overline{T}(u_N)T(u_N)\right]^{N/2}$ from the eigenvalues of $\overline{T}(u_N)T(u_N)$ is a serious problem, because the spectrum is infinitely degenerate in the limit of infinite Trotter number $u_N \to 0$ (for $N\to\infty$). To avoid this difficulty, we transform $\mathrm{Tr}[\overline{T}(u_N)T(u_N)]^{N/2}$ as

$$\begin{aligned}&\mathrm{Tr}\prod_{k=1}^{N/2}\mathrm{Str}_{a_{2k}a_{2k-1}}\{\overline{R}_{a_{2k}L}(u_N)\dots\overline{R}_{a_{2k}1}(u_N)R_{a_{2k-1}L}(u_N)\dots R_{a_{2k-1}1}(u_N)\}\\ &\quad = \mathrm{Str}\prod_{j=1}^{L}\mathrm{Tr}_j\prod_{k=1}^{N/2}\overline{R}_{a_{2k}j}(u_N)R_{a_{2k-1}j}(u_N).\end{aligned} \tag{2.24}$$

Now we introduce the QTM,

$$T_Q(v) = \mathrm{Tr}_j\prod_{k=1}^{N/2}\overline{R}_{a_{2k}j}(u_N+v)R_{a_{2k-1}j}(u_N-v) \tag{2.25}$$

explicitly

$$T_{Q\,\alpha_1\alpha_2\ldots\alpha_N}^{\beta_1\beta_2\ldots\beta_N}(v) = (-)^{\sum_{j=2}^{N}(p[\alpha_j]+p[\beta_j])\sum_{k=1}^{j-1}p[\beta_k]} \times \overline{R}^{\beta_N a}_{\alpha_N\gamma_{N-1}}(u_N+v)R^{\beta_{N-1}\gamma_{N-1}}_{\alpha_{N-1}\gamma_{N-2}}(u_N-v)\ldots\overline{R}^{\beta_2\gamma_2}_{\alpha_2\gamma_1}(u_N+v)R^{\beta_1\gamma_1}_{\alpha_1 a}(u_N-v). \quad (2.26)$$

Due to the GYBE (2.5) and (2.16), the QTM is commutative, i.e.

$$[T_Q(u_N,v),T_Q(u_N,v')]=0. \quad (2.27)$$

We will see that the largest eigenvalue is separated by a gap from the rest of the spectrum for any N persisting in the limit $N\to\infty$ as long as $T>0$. Since the two limits in equation (2.23) can be interchanged (for a proof, see [6, 7]), we take the limit $L\to\infty$ first. As there exists a finite gap between the largest eigenvalue $\Lambda^{\max}(0)$ and the sub-leading eigenvalues $\Lambda^{\mathrm{sub}}(0)$, we can write

$$f=-\lim_{N\to\infty}\frac{1}{\beta}\ln\Lambda^{\max}(0)+2(n_{\mathrm{e}}-1)\mathrm{ch}(\alpha+1)\gamma. \quad (2.28)$$

In this approach, the thermodynamical completeness $-\lim_{\beta\to0}\beta f=\ln 4$ follows easily from $\lim_{N\to\infty}\Lambda^{\max}(0)=4$ which is obvious from the definition of $R(v)$ (2.3) and $\overline{R}(v)$ (2.15).

Most significantly, this method makes it possible to calculate various correlation lengths at finite temperature through the relation

$$\frac{1}{\xi}=-\lim_{N\to\infty}\ln\left|\frac{\Lambda^{\mathrm{sub}}(0)}{\Lambda^{\max}(0)}\right|. \quad (2.29)$$

The QTM can be diagonalized by means of the algebraic Bethe ansatz method. Due to the fact that auxiliary and quantum space are the same $\mathbb{Z}_2$-graded vector space, one can utilize the results for the algebraic Bethe ansatz for the row-to-row transfer matrix case [28, 29, 36]. (The formulation in [28, 36] is based on the non-graded rational ($\gamma=0$) R-matrix which is connected to our graded case by $R^{\gamma\delta}_{\alpha\beta}\to(-)^{p[\gamma]p[\delta]}R^{\gamma\delta}_{\alpha\beta}$. The basic difference between the standard and graded formulation lies in the existence of extra phase factors in the DVF and the BAE.) Replacing the parameters u_N and v by

$$\frac{\gamma}{2}v\to\mathrm{i}v \qquad \frac{\gamma}{2}u_N\to u_N=\frac{\beta\mathrm{sh}(\alpha+1)\gamma}{N} \quad (2.30)$$

and choosing the state $(|1\rangle\otimes_s|4\rangle)^{\otimes_s N/2}$ as the pseudo-vacuum state (reference state), one writes the eigenvalue $\Lambda(v)$ of the QTM in the DVF

$$\Lambda(v)=\phi_1(v)\frac{q_1(v+\frac{\mathrm{i}}{2}\gamma(2\alpha+1))}{q_1(v+\frac{\mathrm{i}}{2}\gamma)}\mathrm{e}^{2\mu\beta}+\phi_2(v)\frac{q_1(v+\frac{\mathrm{i}}{2}\gamma(2\alpha+1))}{q_1(v+\frac{\mathrm{i}}{2}\gamma)}\frac{q_2(v+\mathrm{i}\gamma)}{q_2(v)}\mathrm{e}^{\mu\beta} +\phi_2(v)\frac{q_1(v+\frac{\mathrm{i}}{2}\gamma(2\alpha+1))}{q_1(v-\frac{\mathrm{i}}{2}\gamma)}\frac{q_2(v-\mathrm{i}\gamma)}{q_2(v)}\mathrm{e}^{\mu\beta}+\phi_3(v)\frac{q_1(v+\frac{\mathrm{i}}{2}\gamma(2\alpha+1))}{q_1(v-\frac{\mathrm{i}}{2}\gamma)} \quad (2.31)$$

where the functions $\phi_1(v)$, $\phi_2(v)$ and $\phi_3(v)$ are defined by

$$\begin{aligned}\phi_1(v)&=\left(\frac{\mathrm{sh}(\mathrm{i}v+u_N)\mathrm{sh}(\mathrm{i}v+u_N-\gamma)\mathrm{sh}(\mathrm{i}v-u_N+\alpha\gamma)}{\mathrm{sh}(\mathrm{i}v+u_N-(\alpha+1)\gamma)\mathrm{sh}(\mathrm{i}v+u_N+\alpha\gamma)\mathrm{sh}(\mathrm{i}v-u_N-\alpha\gamma)}\right)^{\frac{N}{2}}\\ \phi_2(v)&=\left(\frac{\mathrm{sh}(\mathrm{i}v-u_N)\mathrm{sh}(\mathrm{i}v+u_N)}{\mathrm{sh}(\mathrm{i}v-u_N-\alpha\gamma)\mathrm{sh}(\mathrm{i}v+u_N-(\alpha+1)\gamma)}\right)^{\frac{N}{2}}\\ \phi_3(v)&=\phi_1(-v)|_{\alpha\to-\alpha-1}\end{aligned} \quad (2.32)$$

and the chemical potential μ (shifted by $\mu+2\mathrm{ch}(\alpha+1)\gamma\to\mu$, see appendix A) have been introduced. The functions $q_1(v)$ and $q_2(v)$ are written in the form

$$q_1(v)=\prod_{j=1}^{n}\sin(v-v_j^{(1)}) \qquad q_2(v)=\prod_{j=1}^{m}\sin(v-v_j^{(2)}) \quad (2.33)$$

where the unknown parameters $\{v_j^{(1)}\}_{j\in\{1,2,\ldots,n\}}$ and $\{v_j^{(2)}\}_{j\in\{1,2,\ldots,m\}}$ are the Bethe ansatz rapidities determined from the BAE

$$\frac{q_2(v_j^{(1)}+\frac{\mathrm{i}}{2}\gamma)}{q_2(v_j^{(1)}-\frac{\mathrm{i}}{2}\gamma)}=-\frac{\phi_1(v_j^{(1)}-\frac{\mathrm{i}}{2}\gamma)}{\phi_2(v_j^{(1)}-\frac{\mathrm{i}}{2}\gamma)}\mathrm{e}^{\beta\mu}\qquad \frac{q_1(v_j^{(2)}+\frac{\mathrm{i}}{2}\gamma)}{q_1(v_j^{(2)}-\frac{\mathrm{i}}{2}\gamma)}=-\frac{q_2(v_j^{(2)}+\mathrm{i}\gamma)}{q_2(v_j^{(2)}-\mathrm{i}\gamma)}. \tag{2.34}$$

To end this section, we emphasize that our QTM is based on the *graded* formulations, which means that the genuine fermionic statistics of the model are properly built into the algebraic structure of the QTM through the Grassmann parity $p[j]$ (see (2.26)). Nevertheless, the DVF and the BAE have quite simple forms. This indicates that the differences between the null and non-null Grassmann parity models in one dimension are embedded into differences of boundary conditions.

3. Nonlinear integral equations

In this section we analyse the eigenvalue $\Lambda(v)$ in DVF form (2.31) by selecting certain auxiliary functions including the information of the BAE. From now on we consider the repulsive case $\alpha > 0$. For the largest eigenvalue, the auxiliary functions and NLIE have been introduced in [31]. For some special eigenvalues with certain symmetries including the largest eigenvalue, one needs only two auxiliary functions [31].

In order to treat the general case, we introduce the following three auxiliary functions:

$$\begin{aligned}
\mathfrak{a}_0(v)&=\left.\frac{\lambda_1(x)(\lambda_3(x)+\lambda_4(x))}{\lambda_2(x)(\lambda_1(x)+\lambda_2(x)+\lambda_3(x)+\lambda_4(x))}\right|_{x=v+\frac{\mathrm{i}}{2}\alpha\gamma} && \mathfrak{A}_0(v)=1+\mathfrak{a}_0(v)\\
\overline{\mathfrak{a}}_0(v)&=\left.\frac{\lambda_2(x)}{\lambda_3(x)+\lambda_4(x)}\right|_{x=v+\frac{\mathrm{i}}{2}\alpha\gamma} && \overline{\mathfrak{A}}_0(v)=1+\overline{\mathfrak{a}}_0(v)\\
\mathfrak{a}_1(v)&=\left.\frac{\lambda_1(x)}{\lambda_2(x)+\lambda_3(x)+\lambda_4(x)}\right|_{x=v+\frac{\mathrm{i}}{2}\alpha\gamma} && \mathfrak{A}_1(v)=1+\mathfrak{a}_1(v)
\end{aligned} \tag{3.1}$$

where the functions $\lambda_j(x)$ denote the jth term in the right-hand side in the DVF (2.31).

These auxiliary functions satisfy certain functional relations. Exploring their analyticity, one transforms these functional relations into a closed set of NLIEs. Here we consider the NLIE for the largest eigenvalue and some sub-leading ones which describe the correlations.

The details of the calculations are deferred to appendices B and C.

3.1. Largest eigenvalues

First we consider the largest eigenvalue. As described above, one finds the NLIE for this eigenvalue in [31]. For completeness we study this case by using the above three auxiliary functions.

The largest eigenvalue belongs to the sector $n = N$ and $m = N/2$ in the BAE (2.34). From numerical calculations with finite Trotter number N, we observe the above auxiliary functions have the following analytical properties: the function $\mathfrak{A}_0(v)$ ($\overline{\mathfrak{A}}_0(v)$) is analytic and non-zero in a finite strip in the lower (upper) half-plane $-\gamma/2 < \mathrm{Im}\, v < 0$ ($0 < \mathrm{Im}\, v < \gamma/2$), and the function $\mathfrak{A}_1(v)$ is analytic and non-zero along the real axis. (In fact, these auxiliary functions have trivial zeros and poles of order $N/2$ which come from the vacuum parts in the DVF. These zeros and poles partly appear in the above 'analyticity strips' and give rise to the leading terms of the NLIEs.) Hereafter we call the region $-\gamma/2 < \mathrm{Im}\, v < \gamma/2$ the 'physical strip'. Due to this analyticity, we can transform the functional relations satisfied by the above auxiliary

functions into NLIEs by using the Fourier transform together with Cauchy's theorem. In this procedure one takes the Trotter limit $N \to \infty$ analytically (see appendix B). Consequently, we obtain the following closed set of NLIE:

$$\begin{aligned}
&\ln \mathfrak{a}_0(v) = \beta\psi(v) + k * \ln \overline{\mathfrak{A}}_0(v) + k * \ln \mathfrak{A}_1(v) + \beta\mu \\
&\ln \overline{\mathfrak{a}}_0(v) = \beta\psi(-v) + \overline{k} * \ln \mathfrak{A}_0(v) + \overline{k} * \ln \mathfrak{A}_1(v) + \beta\mu \\
&\ln \mathfrak{a}_1(v) = \beta(\psi(v) + \psi(-v)) + \bar{k} * \ln \mathfrak{A}_0(v) + k * \ln \overline{\mathfrak{A}}_0(v) + k_1 * \ln \mathfrak{A}_1(v) + 2\beta\mu
\end{aligned} \tag{3.2}$$

with the kernels and leading terms

$$\begin{aligned}
&k(v) = \frac{\mathrm{sh}\gamma}{2\mathrm{sh}(\mathrm{i}v)\mathrm{sh}(\mathrm{i}v - \gamma)} \qquad \overline{k}(v) = k(-v) \qquad k_1(v) = k(v) + \overline{k}(v) \\
&\psi(v) = \frac{\mathrm{sh}^2(\alpha+1)\gamma}{\mathrm{sh}(\mathrm{i}v + \frac{1}{2}\alpha\gamma)\mathrm{sh}(\mathrm{i}v - \frac{1}{2}\gamma(\alpha+2))}
\end{aligned} \tag{3.3}$$

where the symbol $*$ denotes the convolution defined by

$$f * g(v) = \frac{1}{\pi}\int_C f(v-x)g(x)\,\mathrm{d}x = \frac{1}{\pi}\int_{v-C} f(x)g(v-x)\,\mathrm{d}x. \tag{3.4}$$

The integration contours C for convolutions with $\ln \mathfrak{A}_0$, $\ln \overline{\mathfrak{A}}_0$ and $\ln \mathfrak{A}_1$ in (3.2) should be taken by a straight line ranging over a full period π with imaginary part $-\delta$, $+\delta$ and 0 (δ is arbitrary but fixed in the range $0 < \delta < \gamma/2$), respectively. Through the solution to the above NLIE, the largest eigenvalue is expressed by

$$\ln \Lambda^{\max}(v) = \Psi(v) + \zeta * \ln \mathfrak{A}_0(v) + \overline{\zeta} * \ln \overline{\mathfrak{A}}_0(v) + (\zeta + \overline{\zeta}) * \ln \mathfrak{A}_1(v) \tag{3.5}$$

where the kernels $\zeta(v)$, $\overline{\zeta}(v)$ and the leading term $\Psi(v)$ are defined by

$$\Psi(v) = \frac{-2\beta\mathrm{sh}^2((\alpha+1)\gamma)\mathrm{ch}((\alpha+1)\gamma)}{\mathrm{sh}(\mathrm{i}v + (\alpha+1)\gamma)\mathrm{sh}(\mathrm{i}v - (\alpha+1)\gamma)} \qquad \zeta(v) = \frac{-\psi(-v)}{2\mathrm{sh}(\alpha+1)\gamma} \qquad \overline{\zeta}(v) = \zeta(-v). \tag{3.6}$$

From equation (3.2), we find $\overline{\mathfrak{a}}_0(v) = \mathfrak{a}_0(-v)$ and the real function $\mathfrak{a}_1(v)$ is symmetric with respect to both real and imaginary axis. Hence the threefold set of NLIEs (3.2) can be reduced to only two NLIEs which are identical to the ones in [31].

3.2. General NLIE for arbitrary eigenvalues

The sub-leading eigenvalues of the QTM (2.31) are treated in a way similar to the largest eigenvalue. The main difference lies in the existence of additional zeros and poles of the auxiliary functions. Therefore one observes additional terms in the NLIE ('sin' terms). Consequently all correlation functions are characterized by the distribution patterns of these additional zeros or poles.

Often in the case of excited states the second factors in the convolutions are logarithms of periodic functions, however with non-zero winding numbers, $\ln \mathfrak{A}(\pi/2) - \ln \mathfrak{A}(-\pi/2) = 2n\pi\mathrm{i}$ ($n \in \mathbb{Z}$). This gives rise to a second set of additional terms in the NLIE ('cos' terms).

Thus we obtain the following general NLIE with additional terms $\ln \varphi_0(v)$, $\ln \varphi_1(v)$ and $\ln \overline{\varphi}_0(v)$:

$$\begin{aligned}
&\ln \mathfrak{a}_0(v) = \beta\psi(v) + k * \ln \overline{\mathfrak{A}}_0(v) + k * \ln \mathfrak{A}_1(v) + \ln \varphi_0(v) + \beta\mu \\
&\ln \overline{\mathfrak{a}}_0(v) = \beta\psi(-v) + \overline{k} * \ln \mathfrak{A}_0(v) + \overline{k} * \ln \mathfrak{A}_1(v) + \ln \overline{\varphi}_0(v) + \beta\mu \\
&\ln \mathfrak{a}_1(v) = \beta(\psi(v) + \psi(-v)) + \bar{k} * \ln \mathfrak{A}_0(v) + k * \ln \overline{\mathfrak{A}}_0(v) \\
&\qquad\qquad + k_1 * \ln \mathfrak{A}_1(v) + \ln \varphi_1(v) + 2\beta\mu.
\end{aligned} \tag{3.7}$$

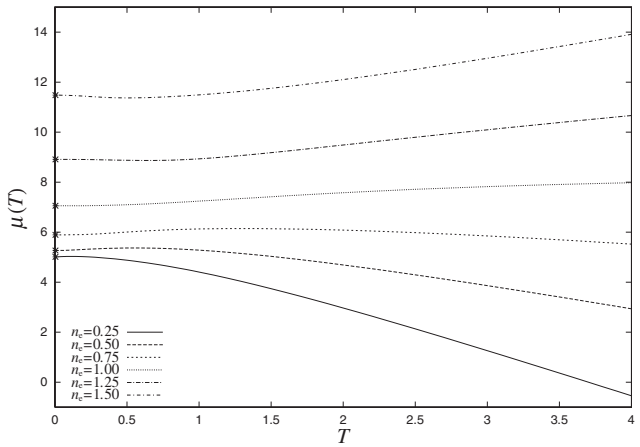

Figure 1. Temperature dependence of the chemical potentials for interaction parameters $\alpha = 1$, $\gamma = 1$ and various particle densities. The symbol $*$ denotes the zero-temperature chemical potentials derived by (A.5) and (A.9) in appendix A. In our units the Boltzmann constant is $k_B = 1$.

The additional terms in the above general NLIE must be determined for each eigenvalue separately. Note that the relation $\varphi_1(v) = \varphi_0(v)\overline{\varphi}_0(v)$ is always valid due to certain algebraic structures of the auxiliary functions (see appendices B and C). In (3.7) and later, we take the same integration contours as in the case of the largest eigenvalue. Thus the corresponding NLIE for arbitrary eigenvalues (including the largest eigenvalue) are written in the following general form:

$$\ln \Lambda(v) = \Psi(v) + \zeta * \ln \mathfrak{A}_0(v) + \overline{\zeta} * \ln \overline{\mathfrak{A}}_0(v) + (\zeta + \overline{\zeta}) * \ln \mathfrak{A}_1(v) + \ln \chi(v) \tag{3.8}$$

where the term $\ln \chi(v)$ is also determined from the distribution pattern of the additional zeros and poles.

As concrete examples, we determine the additional terms for the eigenvalues corresponding to the asymptotics of the (i) one-particle Green function, (ii) transversal spin–spin correlations, (iii) density–density correlations or longitudinal spin–spin correlations, (iv) sub-dominant correlations of case (iii), (v) singlet and (vi) triplet superconducting correlations (see appendix C).

3.3. Numerical analysis of the NLIE

Here we evaluate the above NLIE numerically. As seen in the above section, the NLIEs are exact expressions for the thermodynamical quantities and various correlations at any finite temperature. In contrast to the standard TBA they close at a finite level. Hence one obtains physical quantities explicitly by a highly accurate numerical analysis. To keep the electron density constant, we adopt temperature-dependent chemical potentials $\mu(T)$ determined from

$$\frac{\mathrm{d}\langle n_e(T, \mu(T))\rangle}{\mathrm{d}T} = \frac{\mathrm{d}}{\mathrm{d}T}\left(\frac{\partial f}{\partial \mu}\right)_T = 0. \tag{3.9}$$

In figure 1 we depict $\mu(T)$ for $\alpha = 1$, $\gamma = 1$ and various particle densities. We solve the NLIE by the iteration method. In each step, convolution parts are calculated by making use of the fast Fourier transform. The subsidiary conditions which determine the zeros θ_0, θ_1, etc (see, for example, equation (C.5)) are solved by the Newton method.

Let us consider the NLIE characterizing the correlation lengths via formula (2.29). Figure 2(a) shows the temperature-dependent correlation lengths (multiplied by T) of the one-particle Green functions for various particle densities. The case $\alpha = \gamma = 1$ is used as a concrete example throughout this paper and is equivalent to $U/2 = t_p = 1$ in (1.1). Due to the finite gap of single-particle excitations, we observe that the correlation length multiplied by temperature shows monotonic decay with decreasing temperature with zero limit for zero temperature. We observe a crossover behaviour of the correlation lengths at low temperature close to particle density $n_e = 1.5$: for $n_e < 1.5$ ($n_e > 1.5$) the values of ξ increase (decrease) with n. A similar behaviour is observed in other correlations described by massive excitations. The transversal spin–spin correlations and the triplet superconducting pair correlations are depicted in figures 3(a) and 4(b), respectively. We also depict the temperature-dependent oscillatory terms of the one-particle Green functions, transversal spin–spin correlations, and density–density correlations in figures 2(b), 3(b) and 5(b), respectively. Regarding the one-particle Green functions, one observes clearly a temperature dependence of the 'Fermi momentum' k_F. In the low-temperature limit $T \to 0$, the wavevector converges to the expected value $k_F = \pi n_e/2$ which indicates the significance of the Fermi surface for one-particle excitations in the Tomonaga–Luttinger liquid at $T = 0$. As seen in figure 1 (and also expected) the chemical potential grows to $+\infty$ ($-\infty$) for $T \to \infty$ if the particle density is kept fixed at a high (low) value. This indicates a broadening of the momentum distribution at finite and in particular at high temperatures. Hence, processes of particle–hole type closer to the middle of the band become statistically dominant. Consequently, the wavevector k_F decreases (increases) with increasing T if the value at $T = 0$ is large (small). As shown in figures 5(b) and 3(b), oscillatory terms of the density–density and transversal spin–spin correlations converge to $2k_F \to \pi n_e$. This behaviour corresponds to the excitations carrying a $2k_F$ momentum. For the same reason as mentioned in the case of the one-particle Green function, this $2k_F$ is shifted with increasing temperature. The quantitative difference of the oscillation terms for the transversal spin–spin correlations and the density–density correlations lies in the different nature of these excitations. The density–density correlations are described by particle–hole excitations from the left to the right Fermi point without changing the electron and spin numbers. On the other hand, the transversal spin–spin correlations are characterized by massive excitations changing the spin number.

Figures 5(a) and 4(a) show the density–density and the singlet superconducting pair correlation lengths, respectively. Due to massless excitations, the scaled correlation lengths $T\xi(T)$ are finite at zero temperature. The low-temperature asymptotics agree with the analytic calculations in section 4 and the prediction from CFT in appendix A (see figure A.1). At low temperatures one observes a crossover from dominant density–density correlations to dominant singlet superconducting pair correlations driven by the particle density (see also figure A.1 in appendix A): below (above) a certain critical density ρ_c, the dynamics is dominated by singlet superconducting pair correlations (density–density correlations). This behaviour is changed at higher temperatures. Here at low (high) density ρ the density–density correlations (singlet superconducting pair correlations) dominate, see figure 6. Of course, these findings for high particle density and temperature do not imply any tendency towards superconductivity. It should be borne in mind that the overall length scale of the density–density and singlet superconducting pair correlations is rather short in comparison to the lattice constant. Furthermore, neither of these correlations dominate the dynamics with increasing temperature as the one-particle Green function takes over. This implies a picture of rather uncorrelated one-particle dynamics at higher temperature.

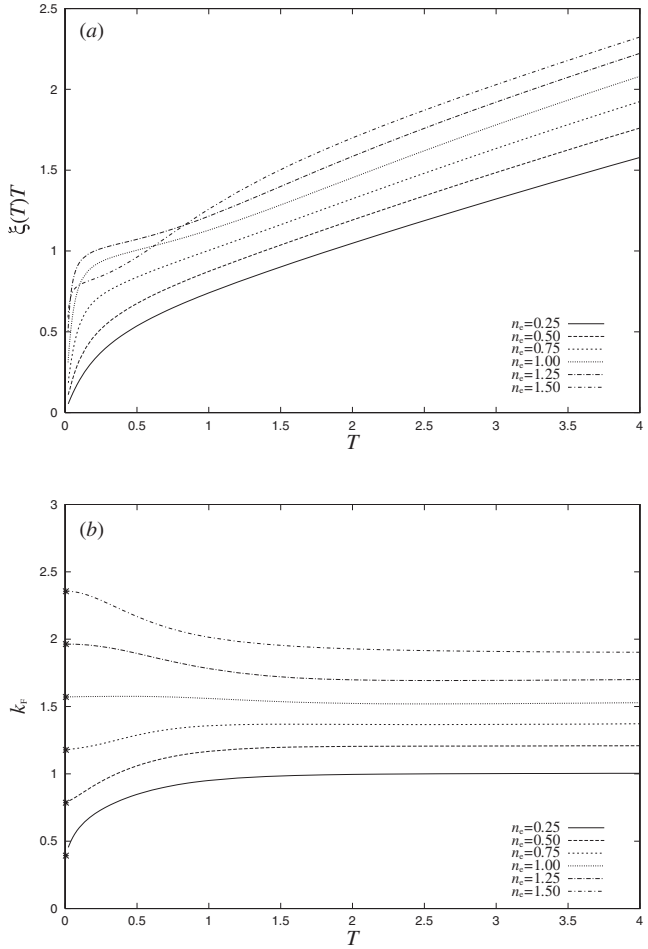

Figure 2. (*a*) Temperature dependence of the scaled correlation lengths $T \cdot \xi(T)$ for the one-particle Green function. (*b*) Temperature dependence of the wavevector of the oscillation terms. At zero temperature one observes the k_F oscillation ($k_F = \pi n_e/2$ depicted by the symbol $*$) characteristic for the one-particle Green function.

Finally, we comment on the sub-dominant density–density (longitudinal spin–spin) correlations in figure 7. The correlations are characterized by simple particle–hole excitations at each Fermi point. Correspondingly, the correlation lengths (multiplied by temperature T) approach the Fermi velocities $v_F/(2\pi)$ in the low-temperature limit.

4. Low-temperature asymptotics

In this section we consider the model at low temperatures. The largest eigenvalue and those sub-leading ones described by massless excitations are calculated approximately up to $O(1/\beta)$. As a consequence, the NLIEs are reduced to only one linear integral equation and this linear integral equation is connected directly with the dressed functions (see appendix A).

Due to the massive spin excitations, the two auxiliary functions $\ln \mathfrak{a}_0(v)$ and $\ln \overline{\mathfrak{a}}_0(v)$ can be neglected as $\mathfrak{a}_0, \overline{\mathfrak{a}}_0 \sim e^{-\epsilon\beta}$ ($\epsilon > 0$). Hence the three NLIEs characterizing the grand

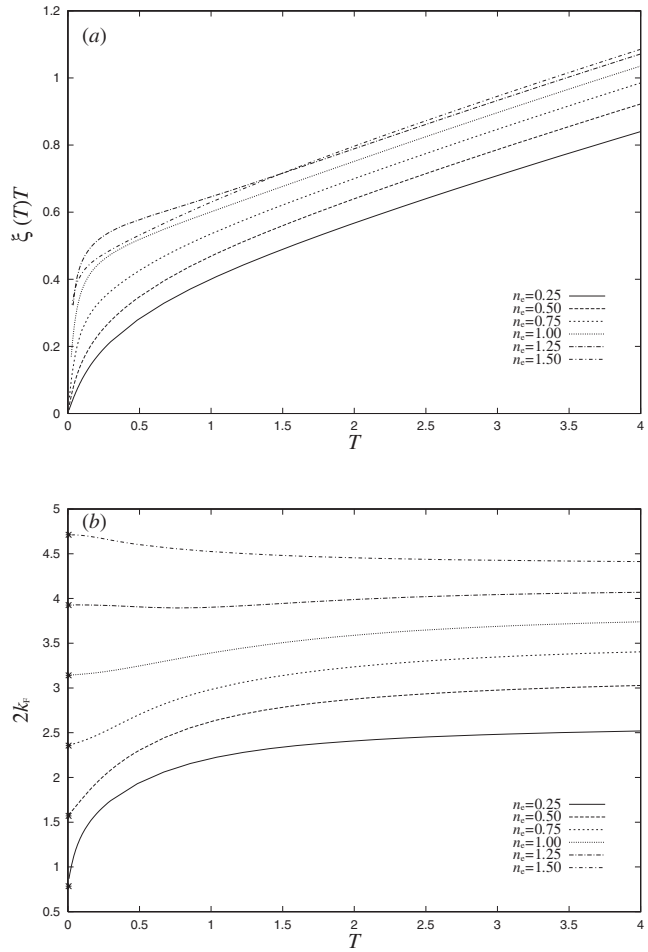

Figure 3. (*a*) Temperature dependence of the correlation lengths of the transversal spin–spin correlations. (*b*) The wavevector $2k_{\mathrm{F}}$ of the oscillations which is characteristic for the spin–spin correlations. At zero temperature one observes the strict relation of wavevector with particle density $2k_{\mathrm{F}} = \pi n_{\mathrm{e}}$ (analytical values are depicted by the symbol $*$).

potential and correlation functions reduce to the single integral equation

$$\ln \mathfrak{a}_1(v) = -\beta\varepsilon^{(0)}(v) + k_1 \overset{C_1}{*} \ln \mathfrak{A}_1(v) + \ln \tilde{\varphi}_1(v) \tag{4.1}$$

where

$$\varepsilon^{(0)}(v) = -\psi(v) - \psi(-v) - 2\mu \tag{4.2}$$

and $\tilde{\varphi}_1$ is a collection of only the 'cos' terms of the function φ_1 listed in appendix C. The 'sin' terms do not show up explicitly as they are taken care of by the modified contour C_1 (see appendix C). Throughout this section the convolution $f * g(v)$ is understood in the manner

$$f * g(v) := \frac{1}{\pi} \int_C f(v-x)g(x)\,\mathrm{d}x. \tag{4.3}$$

Numerically, one observes that the function $\mathfrak{a}_1(v)$ has a crossover behaviour from $\mathfrak{a}_1(v) \ll 1$ to $\mathfrak{a}_1(v) \gg 1$ (see figure 8). The Fermi point Λ_{F} can be defined by the following conditions

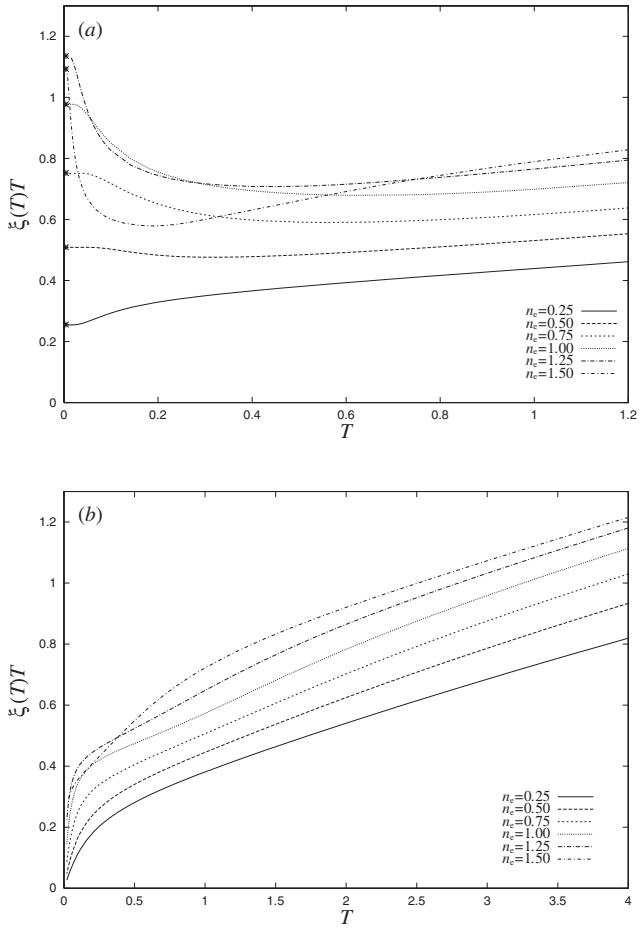

Figure 4. Temperature dependence of the correlation lengths for singlet superconducting pair correlations (*a*) and triplet pair correlations (*b*). The symbol $*$ in (*a*) denotes results of the analytical calculation in the low-temperature limit presented in section 4 confirming the predictions from CFT in appendix A.

satisfied by $\ln \mathfrak{a}_1(v)$ for the largest eigenvalue (C_1 is taken by a straight line on the real axis),

$$\ln \mathfrak{a}_1(\pm\Lambda_{\mathrm{F}}) = 0 \qquad (1/\beta \ll 1) \tag{4.4}$$

and for the excited states we demand $\mathrm{Re}\ \ln \mathfrak{a}_1(\pm\Lambda_{\mathrm{F}}) = 0$ for $\pm\Lambda_{\mathrm{F}}$ on the real axis.

4.1. O(β) *and* O(1) *approximation*

First we calculate O(β) and O(1) approximations for the largest and those sub-leading ones characterized by gapless excitations: (i) particle–hole excitations at each of the left and right Fermi points (define n^+ and n^- as corresponding quantum numbers), (ii) particle–hole excitations of d_{c} charges from the left to right Fermi point, but no change of the total charge number and total spin number, and (iii) singlet pair excitations near the Fermi points; annihilate or create $\Delta N_{\mathrm{c}} = 2n_{\mathrm{c}}$ ($n_{\mathrm{c}} \in \mathbb{Z}$) charges in a symmetric way near the Fermi points. The longitudinal spin–spin correlations $\langle \sigma_j^z \sigma_i^z \rangle$ and the density–density correlations $\langle n_j n_i \rangle$ are

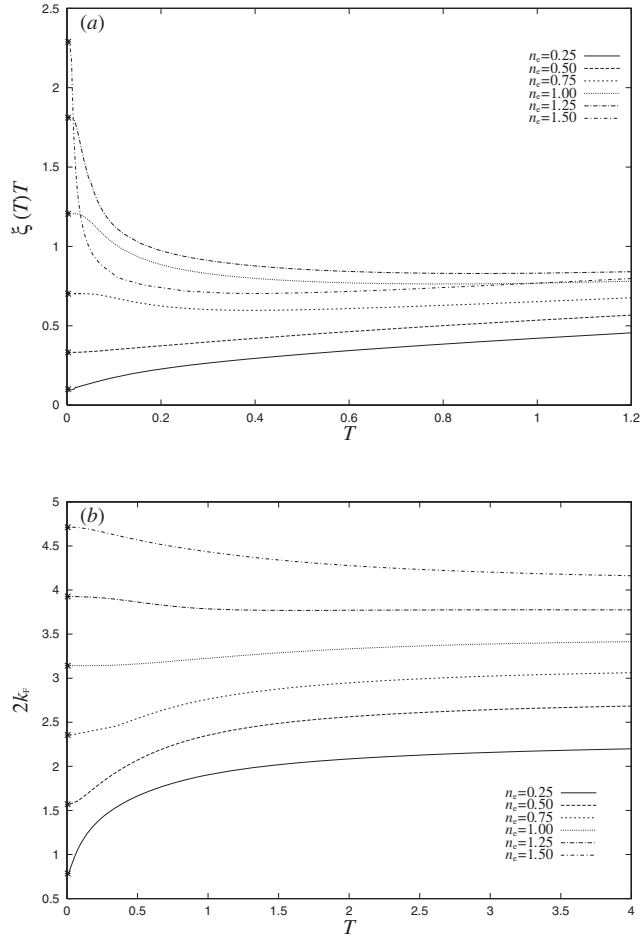

Figure 5. (*a*) Temperature dependence of the correlation lengths for the density–density correlations. The wavevector of the oscillation term is depicted in (*b*). The symbol $*$ denotes results of the analytical calculation in section 4 in the low-temperature limit and the predictions from CFT in appendix A.

characterized by excitations (i) and (ii). On the other hand, the singlet superconducting pair correlations $\langle c_{j+1,\uparrow}c_{j,\downarrow}c_{i+1,\uparrow}c_{i,\downarrow}\rangle$ are described by (iii).

4.1.1. The largest eigenvalue. In the low-temperature limit, the function $\ln \mathfrak{A}_1(v)$ can be written in terms of $\mathfrak{a}_1(v)$ as $\ln \mathfrak{A}_1(v) \simeq \ln \mathfrak{a}_1(v)$ for $|v| > \Lambda_F$ and $\ln \mathfrak{A}_1(v) \simeq 0$ for $|v| < \Lambda_F$ (figure 8). Hence we have

$$\ln \mathfrak{a}_1(v) = -\beta\varepsilon^{(0)}(v) + k_1 \overset{C_1}{*} \ln \mathfrak{a}_1(v) + \mathrm{O}(1/\beta) \tag{4.5}$$

where the symbol $\overset{C_1}{*}$ for the case of the largest eigenvalue denotes

$$\begin{aligned} k_1 \overset{C_1}{*} \ln \mathfrak{a}_1(v) &= \frac{1}{\pi}\int_{C_1} k_1(x) \ln \mathfrak{a}_1(v-x)\,\mathrm{d}x \\ &= \frac{1}{\pi}\left(\int_{-\frac{\pi}{2}}^{-\Lambda_F} + \int_{\Lambda_F}^{\frac{\pi}{2}}\right) k_1(x) \ln \mathfrak{a}_1(v-x)\,\mathrm{d}x. \end{aligned} \tag{4.6}$$

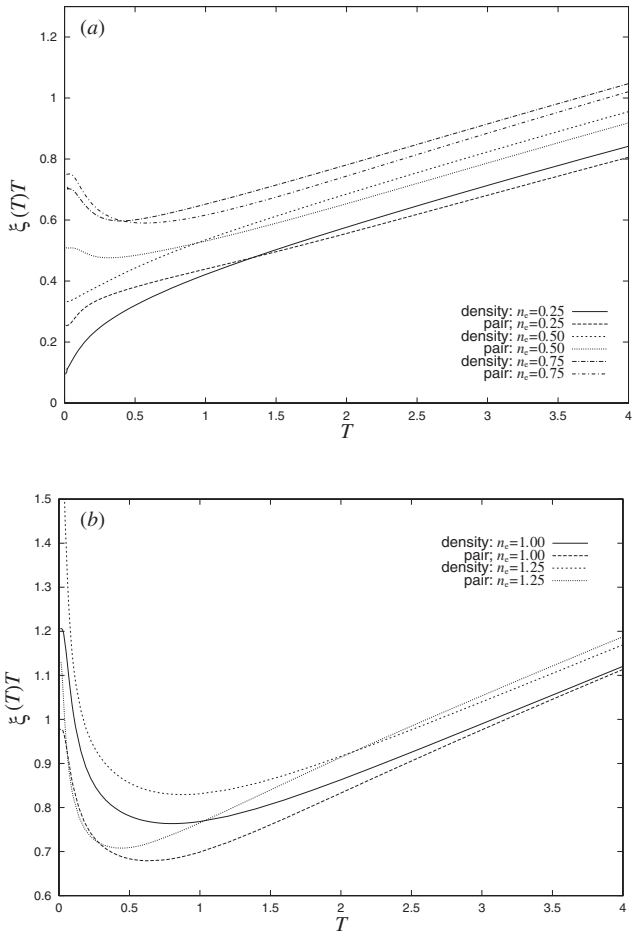

Figure 6. (*a*) Low particle density: crossover from dominant (superconducting) singlet pair correlations at low temperature to dominant density–density correlations at high temperature. (*b*) High particle density: opposite to scenario in (*a*) for density $n = 1.25$ (upper two curves). For $n = 1.0$ the crossing lies outside the shown temperature window.

Using the definition of the dressed energy $\varepsilon(v)$ (A.7), we find a solution to the above equation

$$\ln \mathfrak{a}_1(v) = -\beta\varepsilon(v) + \mathrm{O}(1/\beta). \tag{4.7}$$

Then we have an approximate value for $\ln \mathfrak{a}_1(v)$ at the Fermi points

$$\ln \mathfrak{a}_1(\pm\Lambda_\mathrm{F}) = 0 + \mathrm{O}(1/\beta). \tag{4.8}$$

4.1.2. Particle–hole excitations at each of left and right Fermi points. This excitation is characterized by excited charges at the left (right) Fermi points $-\Lambda_\mathrm{F}$ (Λ_F). In the simplest, still characteristic, case, one zero is separated by n^- (n^+) holes from the Fermi sea of zeros at the Fermi point $\mp\Lambda_\mathrm{F}$. The holes (zeros) are to be circumvented by the deformed contour in anti-clockwise (clockwise) manner (see appendix C). The function $\ln \mathfrak{A}_1(v)$ can be approximated in terms of $\mathfrak{a}_1(v)$ in the same manner as case (1). Hence we obtain the same approximate value as in (4.8).

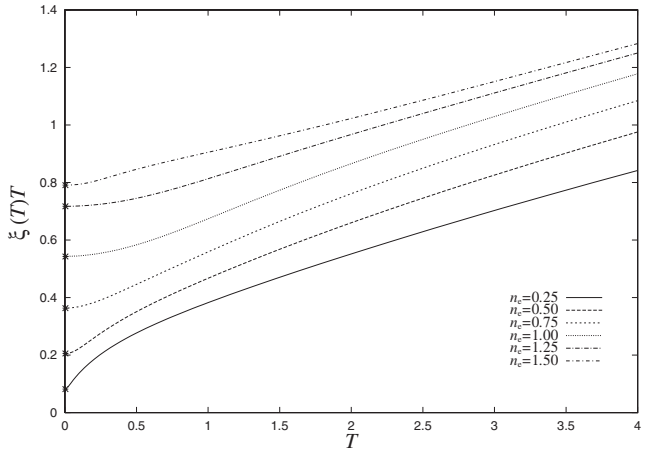

Figure 7. Temperature dependence of the sub-dominant density–density (longitudinal spin–spin) correlation lengths. At low temperature there is convergence to the Fermi velocity $v_F/(2\pi)$ (denoted by the symbol $*$).

4.1.3. Particle–hole excitations from left to right Fermi points. These excitations are described by d_c charges moved from the left (right) Fermi point to right (left) one. This excitation entails a change of momentum $2k_F d_c$. Correspondingly, the auxiliary function $\mathfrak{A}_1(v)$ has $2d_c$ zeros near the Fermi points with behaviour different from those in the largest eigenvalue case: d_c zeros (of 'particle type') are distributed in the upper half-plane near the left Fermi point and the remaining d_c zeros (of 'hole type') are located in the lower half-plane near the right Fermi point, and vice versa.

These zeros should be circumvented by the deformed contours in clockwise manner at the left Fermi point and anti-clockwise manner at the right Fermi point (see appendix C). At low temperatures, $\ln \mathfrak{A}_1(v)$ is replaced by $\ln \mathfrak{A}_1(v) \simeq 0$ for $|v| < \Lambda_F$ and $\ln \mathfrak{A}_1(v) \simeq \ln \mathfrak{a}_1(v) + 2\pi i d_c$ for $|v| > \Lambda_F$ (see figure 9 for $d_c = 1$). Thus we have the linear integral equation characterizing the excitation:

$$\ln \mathfrak{a}_1(v) = -\beta\varepsilon^{(0)}(v) + k_1 \overset{C_1}{*} \ln(\mathfrak{a}_1(v) + 2\pi i d_c) + O(1/\beta) \tag{4.9}$$

where C_1 denotes the integration in the region $|v| > \Lambda_F$ along with the modified contours C_1 defined in appendix C. From the definition of the dressed energy $\varepsilon(v)$ (A.7) and the dressed charge $Z(v)$ (A.12), we have a solution to the above equation,

$$\ln \mathfrak{a}_1(v) = -\beta\varepsilon(v) + \left(\frac{Z(v)}{2} - 1\right) \cdot 2\pi i d_c + O(1/\beta). \tag{4.10}$$

Thus we obtain the value

$$\ln \mathfrak{a}_1(\Lambda_F) = \left(\frac{Z(\Lambda_F)}{2} - 1\right) \cdot 2\pi i d_c + O(1/\beta). \tag{4.11}$$

4.1.4. Singlet pair excitations. As mentioned above, singlet pair excitations are characterized by annihilated $2n_c$ charges. Correspondingly, one observes the function $\mathfrak{A}_1(v)$ has $2n_c$ additional zeros near the Fermi points, i.e. n_c zeros are located near the left Fermi point and remaining n_c zeros are located near the right Fermi point. All these additional zeros are distributed in the lower half-plane and are circumvented by the deformed contour in a manner

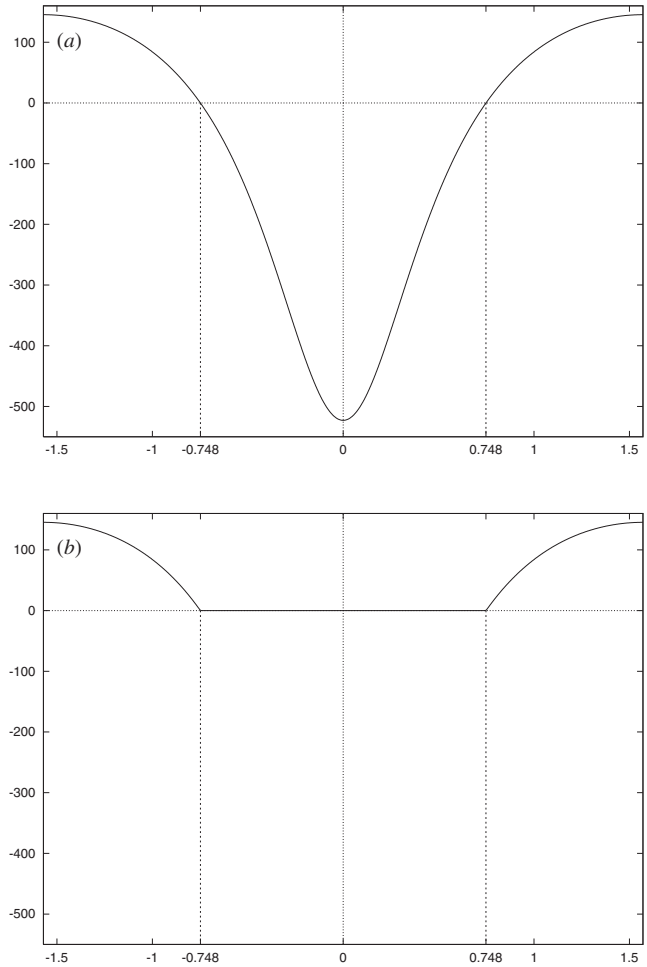

Figure 8. Crossover behaviour of the functions (*a*) $\ln \mathfrak{a}_1(v)$ and (*b*) $\ln \mathfrak{A}_1(v)$ (real parts) for $\alpha = \gamma = 1$, $n_e = 1.00$ and $\beta = 50$. The Fermi point Λ_F defined by (4.4) is found to be $\Lambda_F = \pm 0.748$.

different from case (3), in counter-clockwise manner at both Fermi points (see appendix C). Simultaneously, n_c additional poles appear in the upper half-plane and are located on the $\pi/2$-axis. Though these poles do not appear explicitly in the NLIE, they lead to a non-vanishing winding number of $\mathfrak{a}_1(v)$, i.e. $\ln \mathfrak{a}_1(v)$ is not periodic (see figure 10):

$$\mathrm{Im}\,[\ln \mathfrak{a}_1(\pm\pi/2)] = \mp n_c \pi. \tag{4.12}$$

In the-low temperature limit, $\ln \mathfrak{A}_1(v)$ can be replaced by $\ln \mathfrak{A}_1(v) \simeq 0$ for $|v| < \Lambda_F$, $\ln \mathfrak{A}_1(v) \simeq \ln \mathfrak{a}_1(v) - 2\pi i n_c$ for $-\pi/2 < v < -\Lambda_F$ and $\ln \mathfrak{A}_1(v) \simeq \ln \mathfrak{a}_1(v) + 2\pi i n_c$ for $\Lambda_F < v < \pi/2$ (see figure 10). Thus we obtain the integral equation

$$\ln \mathfrak{a}_1(v) = -\beta \varepsilon_0(v) + k_1 \overset{C_1}{*} S[\ln \mathfrak{a}_1](v) + \mathrm{O}(1/\beta) \tag{4.13}$$

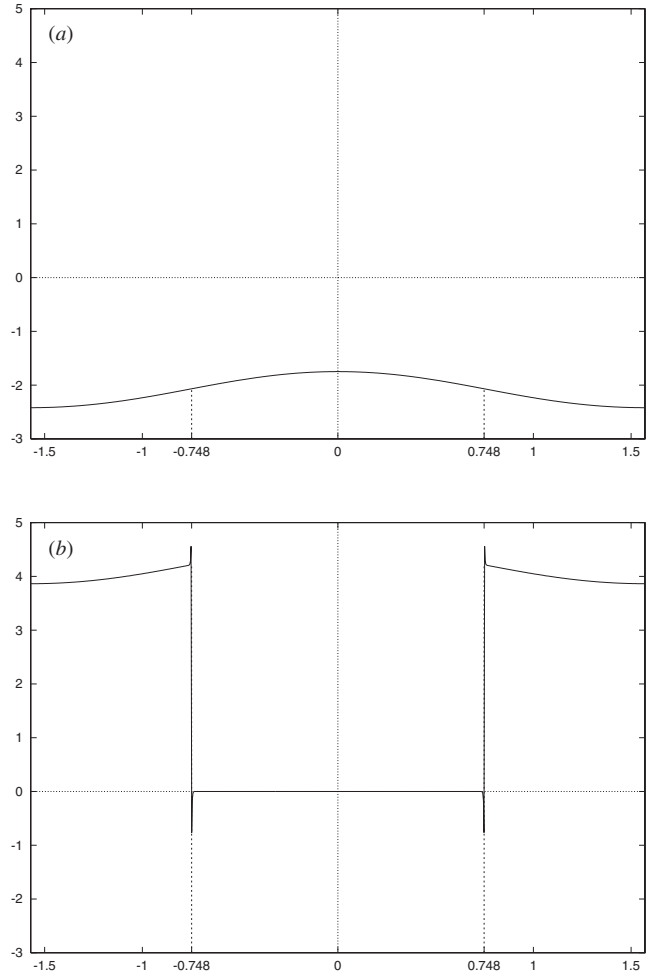

Figure 9. Numerical results for the functions Im $\ln \mathfrak{a}_1(v)$ (*a*) and Im $\ln \mathfrak{A}_1(v)$ (*b*) for $\alpha = \gamma = 1$, $n_e = 1.00$, $\beta = 50$ and $d_c = 1$. Due to the additional zeros (circumvented by the modified integration contour C_1), $\ln \mathfrak{A}_1(v)$ is discontinuous near the Fermi points $\Lambda_F = \pm 0.748$.

where the symbol $\overset{C_1}{*}$ denotes the convolution and the functional $S[g]$ applied to an analytic function $g(v)$ is defined stepwise by

$$S[g](v) = \begin{cases} g(v) - 2\pi i n_c & \text{for} \quad -\pi/2 < v < -\Lambda_F \\ 0 & \text{for} \quad -\Lambda_F < v < \Lambda_F \\ g(v) + 2\pi i n_c & \text{for} \quad \Lambda_F < v < \pi/2 \end{cases} \tag{4.14}$$

with 'analytic continuation' out of the interval $[-\pi/2, \pi/2]$ by the description $S[g](v + \pi) = S[g](v) + 4\pi i n_c$. We directly see that the real part of the solution to (4.13) is given by the dressed energy (A.7)

$$\ln \mathfrak{a}_1(v) = -\beta\varepsilon(v) + i f(v) \tag{4.15}$$

and the imaginary part f has to satisfy the linear integral equation

$$i f(v) = k_1 \overset{C_1}{*} S[i f](v). \tag{4.16}$$

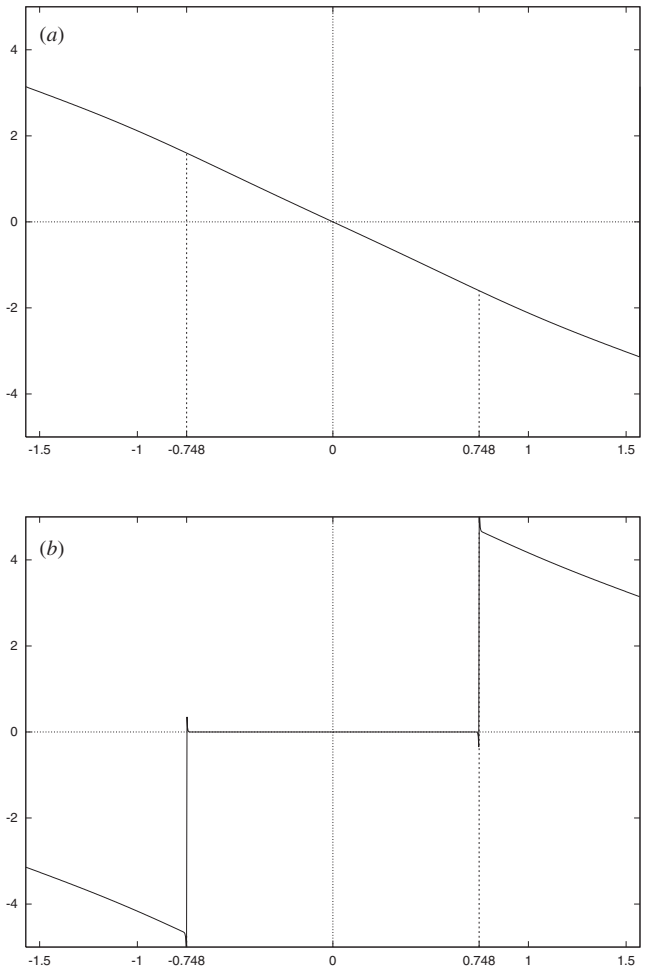

Figure 10. Numerical results for the functions (*a*) Im $\ln \mathfrak{a}_1(v)$ and (*b*) Im $\ln \mathfrak{A}_1(v)$ for $\alpha = \gamma = 1$, $n_e = 1.00$, $\beta = 50$ and $n_c = 1$. One observes that the function $\ln \mathfrak{a}_1(v)$ is a superposition of a periodic function and a linearly increasing term. The function $\ln \mathfrak{A}_1(v)$ is discontinuous at the Fermi points $\Lambda_F = \pm 0.748$. The discontinuity derives from the additional zeros (circumvented by the contour) at the Fermi points.

Obviously, the solution is unique and odd. Taking the derivative of (4.16) we find

$$\begin{aligned} f'(v) &= f_0'(v) + k_1 \overset{C_1}{*} f'(v) \\ f_0'(v) &= \frac{1}{\pi}\big\{k_1(v-\Lambda_F)(f(\Lambda_F)+2n_c\pi) + k_1(v+\Lambda_F)(-f(-\Lambda_F)+2n_c\pi)\big\}. \end{aligned} \tag{4.17}$$

The symbol C_1 denotes the integration contour $[-\pi/2, -\Lambda_F]\bigcup[\Lambda_F, \pi/2]$. From the relation $f(-\pi/2) = -f(\pi/2) = n_c\pi$, we find for the odd function $f(v)$

$$2f(\Lambda_F) + 2n_c\pi = -\int_{C_1} f'(v)\,\mathrm{d}v = -\int_{C_1} \frac{Z(v)f_0'(v)}{2}\,\mathrm{d}v. \tag{4.18}$$

Substituting (4.17) and using the definition of the dressed charge $Z(v)$ (A.12), we arrive at

$$f(\Lambda_F) = \left(\frac{1}{Z(\Lambda_F)} - 1\right)\cdot 2\pi n_c. \tag{4.19}$$

From equation (4.15) and the above result, $\ln \mathfrak{a}_1(\Lambda_F)$ is expressed by

$$\ln \mathfrak{a}_1(\Lambda_F) = \left(\frac{1}{Z(\Lambda_F)} - 1\right) \cdot 2\pi i n_c. \tag{4.20}$$

4.1.5. General cases. Due to linearity and the results in (1)–(4), one finds

$$\ln \mathfrak{a}_1(\Lambda_F) = \left(\frac{Z(\Lambda_F)}{2} - 1\right) \cdot 2\pi i d_c + \left(\frac{1}{Z(\Lambda_F)} - 1\right) \cdot 2\pi i n_c. \tag{4.21}$$

4.2. $O(1/\beta)$ *corrections for the NLIEs*

To evaluate the $O(1/\beta)$ corrections for the NLIEs (4.1), we must calculate the integral term, taking into account its behaviour near the Fermi points $\pm\Lambda_F$. To achieve this, we divide the integration term into three parts as

$$\begin{aligned}
\frac{1}{\pi}\int_{-\frac{\pi}{2}}^{\frac{\pi}{2}} k_1(x)\ln \mathfrak{A}_1(v-x)\,dx &= \int_{-\frac{\pi}{2}}^{\frac{\pi}{2}} k_1(v-x)\ln \mathfrak{A}_1(x)\,dx + n_c \ln\frac{\cos(v+i\gamma)}{\cos(v-i\gamma)} \\
&\to \frac{1}{\pi}\int_{C_1} k_1(v-x)(\ln \mathfrak{a}_1(x) + 2\pi i d_c + 2\pi i\sigma(x))\,dx + n_c \ln\frac{\cos(v+i\gamma)}{\cos(v-i\gamma)} \\
&\quad + \frac{1}{\pi}\int_{C_1} k_1(v-x)\ln\left(1+\frac{1}{\mathfrak{a}_1(x)}\right)dx \\
&\quad + \frac{1}{\pi}\int_{|v|<\Lambda_F} k_1(v-x)\ln(1+\mathfrak{a}_1(x))\,dx
\end{aligned} \tag{4.22}$$

with $\sigma(x) = -n_c, 0, n_c$ for $x \in [-\pi/2, -\Lambda_F], [-\Lambda_F, \Lambda_F], [\Lambda_F, \pi/2]$. Note that the additional 'cos' term which depends on the definition of the convolution (see appendix C) appears in the above equation. As we have already treated the first linear term in equation (4.22), we concentrate on the last two nonlinear terms. Let us split the integration intervals into two parts: $[-\pi/2, 0]\bigcup[0, \pi/2]$. The integrations over the negative interval read

$$\frac{1}{\pi}\int_{-\pi/2}^{-\Lambda_F} k_1(v-x)\ln\left(1+\frac{1}{\mathfrak{a}_1(x)}\right)dx + \frac{1}{\pi}\int_{-\Lambda_F}^{0} k_1(v-x)\ln(1+\mathfrak{a}_1(x))\,dx. \tag{4.23}$$

Changing the variable to $z = -\ln \mathfrak{a}_1(v)$ and using the fact that the derivative of $\ln \mathfrak{a}_1(v)$ is dominated by the one of $-\beta\varepsilon(v)$, i.e. $dz/dv \simeq -\ln' \mathfrak{a}_1(-\Lambda_F) = \beta\varepsilon'(-\Lambda_F) = -\beta\varepsilon'(\Lambda_F)$, one obtains

$$(4.23) = -\frac{k_1(v+\Lambda_F)}{\pi\beta\varepsilon'(\Lambda_F)}\left(\int_{-\ln \mathfrak{a}_1(-\Lambda_F)}^{\infty} \ln(1+e^{-z})\,dz + \int_{-\infty}^{-\ln \mathfrak{a}_1(-\Lambda_F)} \ln(1+e^{z})\,dz\right). \tag{4.24}$$

The integration contours should be taken to circumvent the singularities (see appendix C). The resultant integration is expressed as

$$\to -\frac{k_1(v+\Lambda_F)}{\pi\beta\varepsilon'(\Lambda_F)}\left(\frac{\pi^2}{6} + \frac{1}{2}[\ln \mathfrak{a}_1(-\Lambda_F) + 2\pi i(d_c - n_c)]^2 - 4\pi^2 n^-\right). \tag{4.25}$$

Adding the results of the positive real axis, we obtain

$$\begin{aligned}
&\frac{1}{\pi}\int_{C_1} k_1(v-x)\ln\left(1+\frac{1}{\mathfrak{a}_1(x)}\right)dx + \frac{1}{\pi}\int_{|v|<\Lambda_F} k_1(v-x)\ln(1+\mathfrak{a}_1(x))\,dx \\
&\qquad = \frac{-\pi}{\beta\varepsilon'(\Lambda_F)}\left\{\left(\frac{1}{6} - 4\Delta^+\right)k_1(v-\Lambda_F) + \left(\frac{1}{6} - 4\Delta^-\right)k_1(v+\Lambda_F)\right\}
\end{aligned} \tag{4.26}$$

$$\Delta^{\pm} = \frac{1}{2}\left(\frac{n_c}{Z(\Lambda_F)} \pm \frac{d_c}{2}Z(\Lambda_F)\right)^2 + n^{\pm}.$$

Here $\Delta^{\pm}$ is nothing but the conformal dimensions defined in (A.11). Hence we obtain the NLIE up to $O(1/\beta)$,

$$\ln \mathfrak{a}_1(v) = -\beta\varepsilon^{(0)}(v) + k_1 \overset{C_1}{*} (\ln \mathfrak{a}_1 + 2\pi \mathrm{i} d_c + 2\pi \mathrm{i}\sigma)(v) + n_c \ln \frac{\cos(v+\mathrm{i}\gamma)}{\cos(v-\mathrm{i}\gamma)} - \frac{\pi}{\beta\varepsilon'(\Lambda_F)} \left\{ \left(\frac{1}{6} - 4\Delta^+\right) k_1(v-\Lambda_F) + \left(\frac{1}{6} - 4\Delta^-\right) k_1(v+\Lambda_F) \right\}. \tag{4.27}$$

4.3. $O(1/\beta)$ *corrections to the eigenvalues*

Repeating the same argument for the eigenvalues, we obtain

$$\ln \Lambda(0) = 2\beta \mathrm{ch}(\alpha+1)\gamma - \int_{C_1} \frac{\psi(v)+\psi(-v)}{2\pi \mathrm{sh}(\alpha+1)\gamma} (\ln \mathfrak{a}_1(v) + 2\pi \mathrm{i} d_c)\, \mathrm{d}v + \frac{2\pi\psi(\Lambda_F)(1/6 - 2\Delta^+ - 2\Delta^-)}{\beta\varepsilon'(\Lambda_F)\mathrm{sh}(\alpha+1)\gamma}. \tag{4.28}$$

Next we apply the integral identity for bare (a_0, b_0) and dressed functions (a, b), i.e. if $a = a_0 + k * a$, and $b = b_0 + k * b$ then we have $\int a b_0 = \int a_0 b$. Applying this to equation (4.27) ('$a = \ln \mathfrak{a}_1 + 2\pi \mathrm{i} d_c + 2\pi \mathrm{i}\sigma$') and the density function ('$b = \varrho$') defined in (A.4), we obtain

$$-\int_{C_1} \frac{\psi(v)+\psi(-v)}{2\pi \mathrm{sh}(\alpha+1)\gamma} (\ln \mathfrak{a}_1(v) + 2\pi \mathrm{i} d_c)\, \mathrm{d}v = (\beta\mu + \pi \mathrm{i} d_c) n_e + \frac{\beta}{2} \int_{C_1} (\psi(v)+\psi(-v))\rho(v)\, \mathrm{d}v - \frac{\pi}{2\beta\varepsilon'(\Lambda_F)} \left\{ \left(\frac{1}{6} - 4\Delta^+\right) \int_{C_1} k_1(v-\Lambda_F)\varrho(v)\, \mathrm{d}v + \left(\frac{1}{6} - 4\Delta^-\right) \int_{C_1} k_1(v+\Lambda_F)\varrho(v)\, \mathrm{d}v \right\}. \tag{4.29}$$

Substituting (4.29) for (4.28) and using (A.4), we arrive at

$$\begin{aligned} \ln \Lambda(0) &= -\beta\left\{\varepsilon_0 + 2(n_e - 1)\mathrm{ch}(\alpha+1)\gamma - \mu n_e\right\} - \frac{\pi^2 \varrho(\Lambda_F)(1/6 - 2\Delta^+ - 2\Delta^-)}{\beta\varepsilon'(\Lambda_F)} + \pi \mathrm{i} d_c n_e \\ &= -\beta\{\varepsilon_0 + 2(n_e - 1)\mathrm{ch}(\alpha+1)\gamma - \mu n_e\} + \frac{\pi(1/6 - 2\Delta^+ - 2\Delta^-)}{\beta v_F} + \pi \mathrm{i} d_c n_e \end{aligned} \tag{4.30}$$

where ε_0 and v_F denote the ground state energy per site (A.6) and the Fermi velocity (A.14), respectively. Using (4.30) and (2.29), one obtains the low-temperature asymptotics of the correlation lengths:

$$\xi = \frac{\beta v_F}{2\pi(\Delta^+ + \Delta^-)}. \tag{4.31}$$

From the above calculation and the numerical observation, we can describe the low-temperature behaviour of the grand potential (2.28) and the correlation lengths (2.29) by selecting the 'quantum numbers' (n_c, d_c, n^+, n^-).

4.3.1. Free energy. Selecting the quantum numbers $(n_c, d_c, n^+, n^-) = (0, 0, 0, 0)$, we obtain the $O(1/\beta)$ correction for the grand potential per site (2.28),

$$f = \left\{\varepsilon_0 + 2(n_e - 1)\mathrm{ch}(\alpha+1)\gamma + \mu n_e\right\} - \frac{\pi}{6\beta^2 v_F}. \tag{4.32}$$

This asymptotics agrees with CFT with central charge $c = 1$.

4.3.2. Density–density and longitudinal spin correlations. To obtain the low-temperature asymptotics of the correlation lengths ξ_{d} for the density–density correlations $\langle n_j n_i \rangle$, the selection rules require us to set the quantum numbers to $(n_{\mathrm{c}}, d_{\mathrm{c}}, n^+, n^-) = (0, \pm 1, 0, 0)$. Thus we obtain

$$\xi_{\mathrm{d}} = \frac{2\beta v_{\mathrm{F}}}{\pi Z(\Lambda_{\mathrm{F}})^2}. \tag{4.33}$$

In addition to the above correlation lengths, one observes a $2k_{\mathrm{F}}$ oscillation term in the correlation functions

$$2k_{\mathrm{F}} = \pi n_{\mathrm{e}}. \tag{4.34}$$

In the case of the correlation lengths of the longitudinal spin–spin correlations ξ_{sl}, we have to choose the same quantum numbers as for the density–density correlations. Hence we have

$$\xi_{\mathrm{sl}} = \xi_{\mathrm{d}}. \tag{4.35}$$

4.3.3. Sub-dominant density–density (longitudinal spin) correlations. One also obtains the sub-dominant correlation lengths for the density–density or longitudinal spin–spin correlations which are described by the quantum numbers $(n_{\mathrm{c}}, d_{\mathrm{c}}, n^+, n^-) = (0, 0, 1, 0)$ or $(0, 0, 0, 1)$. The resultant asymptotics of the correlation lengths are given by

$$\xi_{\mathrm{d}}^{\mathrm{sub}} = \xi_{\mathrm{sl}}^{\mathrm{sub}} = \frac{\beta v_{\mathrm{F}}}{2\pi}. \tag{4.36}$$

4.3.4. Singlet superconducting pair correlations. Finally, we consider the low-temperature behaviour of the correlation lengths ξ_{sp} for the singlet superconducting pair correlations $\langle c^\dagger_{j+1,\uparrow} c^\dagger_{j,\downarrow} c_{i+1,\uparrow} c_{i,\downarrow} \rangle$ determined from the quantum numbers $(n_{\mathrm{c}}, d_{\mathrm{c}}, n^+, n^-) = (\pm 1, 0, 0, 0)$. The result reads

$$\xi_{\mathrm{sp}} = \frac{\beta v_{\mathrm{F}} Z(\Lambda_{\mathrm{F}})^2}{2\pi}. \tag{4.37}$$

All these analytical calculations of the low-temperature properties are consistent with the numerical results in the previous section and the predictions from CFT in appendix A.

5. Summary and discussion

In this paper we have investigated the finite-temperature correlations of the strongly correlated electron system in one dimension with $U_q(\mathfrak{sl}(2|1))$-invariance and various types of interaction such as Hubbard and correlating hopping terms. As a consequence we observe a competition of normal versus 'superconducting' correlations. By concrete calculations of the corresponding correlation lengths we have found dominant pair correlations for low particle densities n and temperatures T. In detail, we have found that singlet pair correlation lengths dominate over density–density correlation lengths for low n_{e} and T, but also for high n and T. In the latter case, however, the one-particle Green function dominates over all other correlations.

The computational task was achieved by a first principles approach based on a lattice path integral formulation of the Hamiltonian at finite temperature and the subsequent diagonalization of a suitably defined QTM describing transfer in the chain direction. The BAEs for the leading and next-leading eigenvalues were reformulated in terms of a finite set of NLIEs where the limit of infinite Trotter number could be taken analytically. The NLIEs were solved numerically for arbitrary finite temperature and various particle densities. In the low-temperature limit the analytic investigation confirmed the CFT picture and reproduced the dressed energy and dressed charge formalism known from the finite-size analysis of the $T = 0$ problem.

The QTM was based on $\mathbb{Z}_2$-grading formulations, which reflect the proper fermionic statistics. The formulations are applicable directly to other strongly correlated electron systems.

It is an interesting problem to compare our results for the fermionic system with the ones of the corresponding spin system. The eigenvalues of the QTM constructed by the (null Grassmann parity) R-matrix which satisfies the ordinary YBE are written as

$$\begin{aligned}\Lambda^{\mathrm{spin}}(v) = {} & \phi_1(v)\frac{q_1(v+\frac{\mathrm{i}}{2}\gamma(2\alpha+1))}{q_1(v+\frac{\mathrm{i}}{2}\gamma)}\mathrm{e}^{2\mu\beta} + (-)^{N-n}\phi_2(v)\frac{q_1(v+\frac{\mathrm{i}}{2}\gamma(2\alpha+1))}{q_1(v+\frac{\mathrm{i}}{2}\gamma)}\frac{q_2(v+\mathrm{i}\gamma)}{q_2(v)}\mathrm{e}^{\mu\beta} \\ & +(-)^{N-n}\phi_2(v)\frac{q_1(v+\frac{\mathrm{i}}{2}\gamma(2\alpha+1))}{q_1(v-\frac{\mathrm{i}}{2}\gamma)}\frac{q_2(v-\mathrm{i}\gamma)}{q_2(v)}\mathrm{e}^{\mu\beta} \\ & +\phi_3(v)\frac{q_1(v+\frac{\mathrm{i}}{2}\gamma(2\alpha+1))}{q_1(v-\frac{\mathrm{i}}{2}\gamma)}. \end{aligned} \tag{5.1}$$

Due to the extra factor $(-)^{N-n}$ (N denotes the Trotter number and n is the number of electrons), the one-particle Green function for the original system no longer corresponds to the one for the spin system. Consequently, the characteristic k_{F} oscillations for the one-particle Green function disappear and instead $2k_{\mathrm{F}}$ oscillations will enter the corresponding correlation function in the spin system.

In our work we have provided the framework for a systematic investigation of the correlation lengths at finite temperature with an application to a characteristic set of interaction parameters. We have not yet performed a comprehensive study of the phase diagrams for a wider range of parameters. This remains to be done in a future publication. Also, the effect of a non-vanishing magnetic field remains to be explored. We expect that for the isotropic limit, i.e. $\gamma \to 0$, the 'superconducting regime' in the density–temperature phase diagram will shrink to a point. Also the effect of a magnetic field will lead to similar NLIEs where the chemical potential terms $\beta\mu$ have to be replaced by $\beta(\mu \pm h/2)$ and $2\beta\mu$ remains fixed. The solutions to these NLIEs are expected to break the symmetries of the Bethe ansatz patterns with respect to reflections at the imaginary and/or real axis leading to independent Fermi momenta of spin up and spin down electrons.

Acknowledgments

The authors acknowledge financial support by the Deutsche Forschungsgemeinschaft under grant no Kl 645/3-3. The authors would like to thank F Göhmann, N Kawakami, C Scheeren, M Shiroishi and J Suzuki for useful discussions.

Appendix A. Low-temperature behaviour from CFT

The ground state properties and the long-distance behaviour of some correlation functions have already been investigated in [24] with the aid of the root density method and CFT. Here we slightly modify the formulation of [24] for direct comparison of our results with the prediction from CFT. The ground state properties and low-lying excitations considered here are characterized by the BAE

$$\left[\frac{\sin(\lambda_j+(\frac{\alpha}{2}+1)\gamma\mathrm{i})\sin(\lambda_j+\frac{\alpha}{2}\gamma\mathrm{i})}{\sin(\lambda_j-(\frac{\alpha}{2}+1)\gamma\mathrm{i})\sin(\lambda_j-\frac{\alpha}{2}\gamma\mathrm{i})}\right]^L = \prod_{k=1}^{N_\downarrow}\frac{\sin(\lambda_j-\Lambda_k+\mathrm{i}\gamma)}{\sin(\lambda_j-\Lambda_k-\mathrm{i}\gamma)}$$

$$\prod_{j=1}^{N_e/2}\frac{\sin(\Lambda_k-\lambda_j+i\gamma)}{\sin(\Lambda_k-\lambda_j-i\gamma)}=-\prod_{l=1}^{N_\downarrow}\frac{\sin(\Lambda_k-\Lambda_l+i\gamma)}{\sin(\Lambda_k-\Lambda_l-i\gamma)}, \tag{A.1}$$

where N_e and $N_\downarrow$ denote the total number of electrons and the number of down-spin electrons, respectively. We derive directly the above equation from the fact that the ground state energy is described by two-string electron rapidities, and hence shifting the rapidities $\lambda_j \to \lambda_j + i\gamma/2$, $\lambda_{j+1} \to \lambda_j - i\gamma/2$ in equation (6) in [24]. The ground state energy can be written as

$$\begin{aligned} E_0 &= -2\sum_{j=1}^{N_e/2}[\cos(k(\lambda_j+i\gamma/2))+\cos(k(\lambda_j-i\gamma/2))] \\ &= -2\sum_{j=1}^{N_e/2}\left[2\mathrm{ch}(\alpha+1)\gamma+\frac{\psi(\lambda_j)+\psi(-\lambda_j)}{2}\right] \end{aligned} \tag{A.2}$$

where

$$k(v)=\pi-2\arctan\left(\frac{\tan v}{\mathrm{th}((\alpha+1)\gamma/2)}\right). \tag{A.3}$$

By solving the spin rapidities Λ_k in terms of the charge rapidities λ_j, we obtain the density function $\varrho(v)$ in the thermodynamic limit,

$$\varrho(v)=-\frac{\psi(v)+\psi(-v)}{\pi\,\mathrm{sh}(\alpha+1)\gamma}+\frac{1}{\pi}\int_{C_1}k_1(v-x)\varrho(x)\,dx \tag{A.4}$$

where the Fermi points $\pm\Lambda_F$ are determined from the subsidiary condition for the total electron density n_e

$$\int_{C_1}\varrho(x)\,dx=n_e. \tag{A.5}$$

Hence the ground state energy per site ε_0 is expressed in terms of the density function

$$\varepsilon_0=-\int_{C_1}\left(2\mathrm{ch}(\alpha+1)\gamma+\frac{\psi(x)+\psi(-x)}{2}\right)\varrho(x)\,dx. \tag{A.6}$$

The dressed energy $\varepsilon(v)$

$$\varepsilon(v)=\varepsilon^{(0)}(v)+\frac{1}{\pi}\int_{C_1}k_1(v-x)\varepsilon(x)\,dx \tag{A.7}$$

characterizes the low-lying excitations. Here the bare energy function $\varepsilon^{(0)}(v)$ is defined by (as in (A.8))

$$\varepsilon^{(0)}(v)=-\psi(v)-\psi(-v)-2\mu. \tag{A.8}$$

Note that the chemical potential is shifted by $\mu+2\mathrm{ch}(\alpha+1)\gamma \to \mu$. The condition

$$\varepsilon(\pm\Lambda_F)=0 \tag{A.9}$$

provides another way to define the Fermi points $\pm\Lambda_F$ for given chemical potential μ.

As mentioned in section 4, we observe massless excitations described by quantum numbers (n_c, d_c, n^+, n^-). Using the concept of CFT, one obtains the correlation functions for primary fields as

$$\langle\phi_{\Delta^\pm}(x)\phi_{\Delta^\pm}(0)\rangle=\frac{\exp(-2id_ck_F)}{x^{2(\Delta^+\pm\Delta^-)}} \tag{A.10}$$

where $\Delta^\pm$ are the conformal dimensions of the primary operators

$$\Delta^\pm=\frac{1}{2}\left(\frac{n_c}{Z(\Lambda_F)}\pm\frac{d_c}{2}Z(\Lambda_F)\right)^2+n^\pm. \tag{A.11}$$

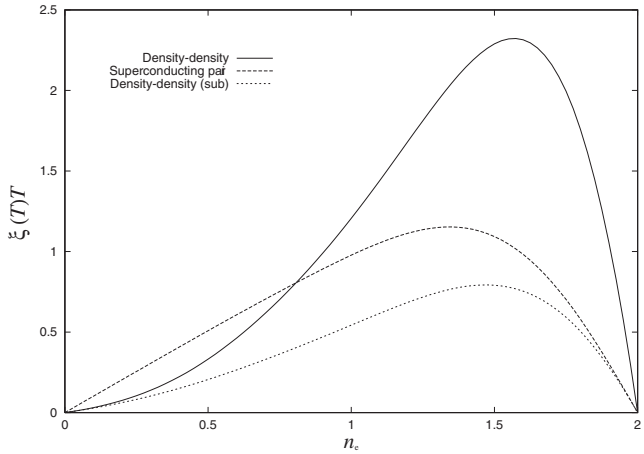

Figure A.1. Numerical results for the correlations based on CFT ($T \ll 1$). The density–density correlations, singlet superconducting pair correlations and the sub-dominant density–density correlations correspond to the quantum numbers $(n_c, d_c, n^+, n^-) = (0, \pm 1, 0, 0)$, $(\pm 1, 0, 0, 0)$ and $(0, 0, 1, 0)$ $((0, 0, 0.1))$, respectively.

Here the function $Z(\Lambda_F)$ denotes the dressed charge determined from the integral equation

$$Z(v) = 2 + \frac{1}{\pi}\int_{C_1} k_1(v-x)Z(x)\,\mathrm{d}x. \tag{A.12}$$

For finite temperatures in the scaling limit ($0 < T \ll 1$), where conformal invariance is valid, the correlation functions are obtained from the $T = 0$ case by the following replacement [5] in (A.10):

$$x \to \frac{v_F\beta}{\pi}\mathrm{sh}\frac{\pi x}{\beta v_F} \tag{A.13}$$

where v_F is the Fermi velocity defined by

$$v_F = \frac{\varepsilon'(-\Lambda_F)}{\pi\varrho(v)} = -\frac{\varepsilon'(\Lambda_F)}{\pi\varrho(v)}. \tag{A.14}$$

Thus the long-distance behaviour of the correlation functions $G(x)$ is given by

$$G(x) \sim \cos(2k_F d_c x)\exp\left(-\frac{2\pi(\Delta^+ + \Delta^-)x}{\beta v_F}\right). \tag{A.15}$$

Fitting this with $G(x) \sim \exp(-x/\xi)$, one obtains the correlation lengths ξ at $T \ll 1$

$$\xi = \frac{\beta v_F}{2\pi(\Delta^+ + \Delta^-)}. \tag{A.16}$$

The numerical results of (A.16) are shown in figure A.1 for $(n_c, d_c, n^+, n^-) = (0, \pm 1, 0, 0)$, $(\pm 1, 0, 0, 0)$ and $(0, 0, 1, 0)$ $((0, 0, 0, 1))$. These low-temperature asymptotics of the correlation lengths are consistent with (4.31).

Appendix B. Derivation of NLIE for largest eigenvalue

Here we derive the NLIE for the largest eigenvalue by using the auxiliary functions defined by (3.1). The derivation is applicable to the general eigenvalues after a simple modification of the integration contours.

The auxiliary functions are defined by certain combinations of $\lambda_j(x)$ $(1 \leqslant j \leqslant 4)$:

$$\begin{aligned}
\mathfrak{a}_0(v) &= \frac{\lambda_1(x)(\lambda_3(x)+\lambda_4(x))}{\lambda_2(x)\Lambda(x)} & \mathfrak{A}_0(v) &= \frac{(\lambda_1(x)+\lambda_2(x))(\lambda_2(x)+\lambda_3(x)+\lambda_4(x))}{\lambda_2(x)\Lambda(x)} \\
\overline{\mathfrak{a}}_0(v) &= \frac{\lambda_2(x)}{\lambda_3(x)+\lambda_4(x)} & \overline{\mathfrak{A}}_0(v) &= \frac{\lambda_2(x)+\lambda_3(x)+\lambda_4(x)}{\lambda_3(x)+\lambda_4(x)} \\
\mathfrak{a}_1(v) &= \frac{\lambda_1(x)}{\lambda_2(x)+\lambda_3(x)+\lambda_4(x)} & \mathfrak{A}_1(v) &= \frac{\Lambda(x)}{\lambda_2(x)+\lambda_3(x)+\lambda_4(x)}
\end{aligned} \tag{B.1}$$

where $x = v + \frac{\mathrm{i}}{2}\alpha\gamma$. Note that the eigenvalues are written in the following form:

$$\Lambda(v) = \lambda_1(v) + \lambda_2(v) + \lambda_3(v) + \lambda_4(v). \tag{B.2}$$

Using the definition of $\lambda_j(x)$, we can write

$$\lambda_1(x) + \lambda_2(x) = \frac{q_1(x + \frac{\mathrm{i}}{2}\gamma(2\alpha+1))}{q_1(x+\frac{\mathrm{i}}{2}\gamma)} \left\{ \phi_1(x)\mathrm{e}^{2\mu\beta} + \phi_2(v)\frac{q_2(x+\mathrm{i}\gamma)}{q_2(x)}\mathrm{e}^{\mu\beta} \right\}. \tag{B.3}$$

One finds that function (B.3) has poles stemming from $q_2(x)$. Due to the BAE (2.34), the poles from $q_1(x + \frac{\mathrm{i}}{2}\gamma)$ must be cancelled out. Hence the second factor in (B.3) must take the following form:

$$\begin{aligned}
&\phi_1(x)\mathrm{e}^{2\mu\beta} + \phi_2(v)\frac{q_2(x+\mathrm{i}\gamma)}{q_2(x)}\mathrm{e}^{\mu\beta} \propto \frac{\mathrm{sh}^{\frac{N}{2}}(\mathrm{i}x + u_N)q_1(x+\frac{\mathrm{i}}{2}\gamma)q_2^h(x)}{\phi_+(x)\mathrm{sh}^{\frac{N}{2}}(\mathrm{i}x - u_N - \alpha\gamma)q_2(x)} \\
&\phi_+(x) = [\mathrm{sh}(\mathrm{i}x + u_N + \alpha\gamma)\mathrm{sh}(\mathrm{i}x + u_N - (\alpha+1)\gamma)]^{\frac{N}{2}}.
\end{aligned} \tag{B.4}$$

where the function $q_2^h(x)$ is a certain analytic function which has $N + m - n$ zeros for the largest eigenvalue case. Substituting (B.4) for (B.3), we obtain

$$\lambda_1(x) + \lambda_2(x) \propto \frac{\mathrm{sh}^{\frac{N}{2}}(\mathrm{i}x + u_N)q_1(x+\frac{\mathrm{i}}{2}\gamma(2\alpha+1))q_2^h(x)}{\phi_+(x)\mathrm{sh}^{\frac{N}{2}}(\mathrm{i}x - u_N - \alpha\gamma)q_2(x)}. \tag{B.5}$$

Similarly, we find that $\lambda_3(x) + \lambda_4(x)$ can be written as

$$\begin{aligned}
&\lambda_3(x) + \lambda_4(x) \propto \frac{\mathrm{sh}^{\frac{N}{2}}(\mathrm{i}x - u_N)q_1(x+\frac{\mathrm{i}}{2}\gamma(2\alpha+1))q_2^h(x-\mathrm{i}\gamma)}{\phi_-(x)\mathrm{sh}^{\frac{N}{2}}(\mathrm{i}x + u_N - (\alpha+1)\gamma)q_2(x)} \\
&\phi_-(x) = [\mathrm{sh}(\mathrm{i}x - u_N - \alpha\gamma)\mathrm{sh}(\mathrm{i}x - u_N + (\alpha+1)\gamma)]^{\frac{N}{2}}.
\end{aligned} \tag{B.6}$$

Thanks to the BAE (2.34), the eigenvalues (B.2) are analytic functions (except for the trivial poles which derive from the vacuum functions in (2.31)). Thus the eigenvalues (B.2) must take the form

$$\Lambda(x) \propto \frac{q_1(v + \frac{\mathrm{i}}{2}\gamma(2\alpha+1))q_1^h(x)}{\phi_+(x)\phi_-(x)} \tag{B.7}$$

where $q_1^h(x)$ is an analytic function having $2N - n$ zeros for the largest eigenvalue case. After shifting the parameter $x \to v + \frac{\mathrm{i}}{2}\alpha\gamma$, we obtain the functional relations to be satisfied by

certain combinations of the auxiliary functions

$$\begin{aligned}
\mathfrak{a}_0(v) &\propto \frac{[\mathrm{sh}(\mathrm{i}v - u_N + \frac{\gamma}{2}\alpha)\mathrm{sh}(\mathrm{i}v + u_N - \frac{\gamma}{2}(\alpha+2))]^{\frac{N}{2}} q_2^h(v + \frac{\mathrm{i}}{2}\gamma(\alpha-2))}{q_1^h(v + \frac{\mathrm{i}}{2}\alpha\gamma) q_2(v + \frac{\mathrm{i}}{2}\gamma(\alpha+2))} \\
\overline{\mathfrak{a}}_0(v) &\propto \frac{[\mathrm{sh}(\mathrm{i}v + u_N - \frac{\gamma}{2}\alpha)\mathrm{sh}(\mathrm{i}v - u_N + \frac{\gamma}{2}(\alpha+2))]^{\frac{N}{2}} q_2(v + \frac{\mathrm{i}}{2}\gamma(\alpha+2))}{q_1(v + \frac{\mathrm{i}}{2}\gamma(\alpha+1)) q_2^h(v + \frac{\mathrm{i}}{2}\gamma(\alpha-2))} \\
\frac{\mathfrak{A}_1(v)}{\mathfrak{a}_1(v)} &\propto \frac{q_1(v + \frac{\mathrm{i}}{2}\gamma(\alpha+1)) q_1^h(v + \frac{\mathrm{i}}{2}\alpha\gamma)}{\phi_+(v + \frac{\mathrm{i}}{2}\alpha\gamma)\phi_-(v + \frac{\mathrm{i}}{2}\alpha\gamma)} \\
\mathfrak{A}_0(v)\mathfrak{A}_1(v) &\propto \frac{q_1(v + \frac{\mathrm{i}}{2}\gamma(\alpha+1)) q_2^h(v + \frac{\mathrm{i}}{2}\gamma\alpha)}{[\mathrm{sh}(\mathrm{i}v + u_N + \frac{\gamma}{2}\alpha)\mathrm{sh}(\mathrm{i}v - u_N - \frac{\gamma}{2}\alpha)]^{\frac{N}{2}} q_2(v + \frac{\mathrm{i}}{2}\gamma(\alpha+2))} \\
\overline{\mathfrak{A}}_0(v)\mathfrak{A}_1(v) &\propto \frac{q_1^h(v + \frac{\mathrm{i}}{2}\gamma\alpha) q_2(v + \frac{\mathrm{i}}{2}\gamma\alpha)}{[\mathrm{sh}(\mathrm{i}v + u_N + \frac{\gamma}{2}\alpha)\mathrm{sh}(\mathrm{i}v - u_N - \frac{\gamma}{2}\alpha)]^{\frac{N}{2}} q_2^h(v + \frac{\mathrm{i}}{2}\gamma(\alpha+2))}.
\end{aligned} \tag{B.8}$$

For the largest eigenvalue, we find numerically the following analyticity properties: $q_1(v + \frac{\mathrm{i}}{2}\gamma(\alpha+1))$, $q_2(v + \frac{\mathrm{i}}{2}\gamma(\alpha+2)$ ($q_1^h(v + \frac{\mathrm{i}}{2}\alpha\gamma)$, $q_2^h(v + \frac{\mathrm{i}}{2}\gamma(\alpha-2))$) are analytic and non-zero in the upper (lower) half-plane, and $\lambda_2(v + \frac{\mathrm{i}}{2}\gamma) + \lambda_3(v + \frac{\mathrm{i}}{2}\gamma) + \lambda_4(v + \frac{\mathrm{i}}{2}\gamma)$ is analytic and non-zero in the physical strip $-\frac{\gamma}{2} < \mathrm{Im}\, v < \frac{\gamma}{2}$. (In fact, we also observe that $q_1^h(v + \frac{\mathrm{i}}{2}\alpha\gamma) = q_1(-v + \frac{\mathrm{i}}{2}\gamma(\alpha+1))$ and $q_2^h(v + \frac{\mathrm{i}}{2}\gamma(\alpha-2)) = q_2(-v + \frac{\mathrm{i}}{2}\gamma(\alpha+2))$ are valid in the largest eigenvalue case and some special sub-leading ones.)

Because of these analyticity properties, we can take the logarithmic derivative and perform the Fourier transform on both sides of (B.8). Explicitly we find

$$\hat{\mathfrak{a}}_0 = \begin{cases} -\hat{q}_1^h \mathrm{e}^{-k\gamma\alpha} + \hat{q}_2^h \mathrm{e}^{-k\gamma(\alpha-2)} + E\left(\frac{\gamma}{2}\alpha - u_N\right) & \text{for} \quad k > 0 \\ -\hat{q}_2 \mathrm{e}^{k\gamma(\alpha+2)} - E\left(-\frac{\gamma}{2}(\alpha+2) + u_N\right) & \text{for} \quad k < 0 \\ -\hat{q}_1^h + \hat{q}_2^h - \hat{q}_2 & \text{for} \quad k = 0 \end{cases}$$

$$\hat{\overline{\mathfrak{a}}}_0 = \begin{cases} -\hat{q}_2^h \mathrm{e}^{-k\gamma(\alpha-2)} + E\left(\frac{\gamma}{2}(\alpha+2) - u_N\right) & \text{for} \quad k > 0 \\ -\hat{q}_1 \mathrm{e}^{k\gamma(\alpha+1)} + \hat{q}_2 \mathrm{e}^{k\gamma(\alpha+2)} - E\left(-\frac{\gamma}{2}\alpha + u_N\right) & \text{for} \quad k < 0 \\ -\hat{q}_2^h - \hat{q}_1 + \hat{q}_2 & \text{for} \quad k = 0 \end{cases}$$

$$\hat{\mathfrak{A}}_1 - \hat{\mathfrak{a}}_1 = \begin{cases} \hat{q}_1^h \mathrm{e}^{-k\gamma\alpha} - E\left(\frac{\gamma}{2}\alpha - u_N\right) - E\left(\frac{\gamma}{2}(\alpha+2) - u_N\right) & \text{for} \quad k > 0 \\ \hat{q}_1 \mathrm{e}^{k\gamma(\alpha+1)} + E\left(-\frac{\gamma}{2}\alpha + u_N\right) + E\left(-\frac{\gamma}{2}(\alpha+2) + u_N\right) & \text{for} \quad k < 0 \\ \hat{q}_1^h + \hat{q}_1 & \text{for} \quad k = 0 \end{cases} \tag{B.9}$$

$$\hat{\mathfrak{A}}_0 + \hat{\mathfrak{A}}_1 = \begin{cases} \hat{q}_2^h \mathrm{e}^{-k\gamma\alpha} - E\left(\frac{\gamma}{2}\alpha + u_N\right) & \text{for} \quad k > 0 \\ \hat{q}_1 \mathrm{e}^{k\gamma(\alpha+1)} - \hat{q}_2 \mathrm{e}^{k\gamma(\alpha+2)} + E\left(-\frac{\gamma}{2}\alpha - u_N\right) & \text{for} \quad k < 0 \\ \hat{q}_2^h + \hat{q}_1 - \hat{q}_2 & \text{for} \quad k = 0 \end{cases}$$

$$\hat{\overline{\mathfrak{A}}}_0 + \hat{\mathfrak{A}}_1 = \begin{cases} \hat{q}_1^h \mathrm{e}^{-k\gamma\alpha} - \hat{q}_2^h \mathrm{e}^{-k\gamma(\alpha+2)} - E\left(\frac{\gamma}{2}\alpha + u_N\right) & \text{for} \quad k > 0 \\ \hat{q}_2 \mathrm{e}^{k\gamma\alpha} + E\left(-\frac{\gamma}{2}\alpha - u_N\right) & \text{for} \quad k < 0 \\ \hat{q}_1^h - \hat{q}_2^h + \hat{q}_2 & \text{for} \quad k = 0 \end{cases}$$

where we have adopted the notation $\hat{f}$ for the Fourier transform of the logarithmic derivative of a function $f(v)$,

$$\hat{f} = \frac{1}{\pi}\int_{-\frac{\pi}{2}}^{\frac{\pi}{2}} \left\{\frac{\partial}{\partial v}\ln f(v)\right\} \mathrm{e}^{2\mathrm{i}kv}\,\mathrm{d}v \qquad \frac{\partial}{\partial v}\ln f(v) = \sum_{k=-\infty}^{\infty} \hat{f}\mathrm{e}^{-2\mathrm{i}kv} \tag{B.10}$$

and $E(x) := \mathrm{i}N\mathrm{e}^{-2kx}$. Applying this procedure to the eigenvalue (B.2), we have

$$\hat{\Lambda} = \begin{cases} \hat{q}_1^h - E((\alpha+1)\gamma - u_N) - E(\alpha\gamma + u_N) & \text{for} \quad k > 0 \\ \hat{q}_1 \mathrm{e}^{k\gamma(2\alpha+1)} + E(-(\alpha+1)\gamma + u_N) + E(-\alpha\gamma - u_N) & \text{for} \quad k < 0 \\ \hat{q}_1^h + \hat{q}_1^h & \text{for} \quad k = 0. \end{cases} \tag{B.11}$$

From the last two equations in (B.9), we find the Fourier modes $\hat{q}_1$, $\hat{q}_2$, $\hat{q}_1^h$ and $\hat{q}_2^h$ can be expressed in terms of $\hat{\mathfrak{A}}_0$, $\hat{\overline{\mathfrak{A}}}_0$ and $\hat{\mathfrak{A}}_1$. Substituting them for the first three equations in (B.9) and integrating over v after performing the inverse Fourier transform (B.10), we arrive at

$$\begin{aligned} \ln \mathfrak{a}_0(v) &= \psi_N(v) + k_0 * \ln \overline{\mathfrak{A}}_0(v) + k_0 * \ln \mathfrak{A}_1(v) + \beta\mu \\ \ln \overline{\mathfrak{a}}_0(v) &= \psi_N(-v) + \overline{k}_0 * \ln \mathfrak{A}_0(v) + \overline{k}_0 * \ln \mathfrak{A}_1(v) + \beta\mu \\ \ln \mathfrak{a}_1(v) &= \psi_N(v) + \psi_N(-v) + \overline{k}_0 * \ln \mathfrak{A}_0(v) + k_0 * \ln \overline{\mathfrak{A}}_0(v) + k_1 * \ln \mathfrak{A}_1(v) + 2\beta\mu \\ \psi_N(v) &= \frac{N}{2} \ln \frac{\mathrm{sh}(\mathrm{i}v - u_N + \frac{\gamma}{2}\alpha)\mathrm{sh}(\mathrm{i}v + u_N - \frac{\gamma}{2}(\alpha+2))}{\mathrm{sh}(\mathrm{i}v + u_N + \frac{\gamma}{2}\alpha)\mathrm{sh}(\mathrm{i}v - u_N - \frac{\gamma}{2}(\alpha+2))} \end{aligned} \tag{B.12}$$

where the integration contours for the convolutions with $\ln \mathfrak{A}_0$, $\ln \overline{\mathfrak{A}}_0$ and $\ln \mathfrak{A}_1$ are taken by the straight line with the imaginary part $-\delta$, $+\delta$ and 0 (δ is arbitrary but fixed in the range $0 < \delta < \gamma/2$), respectively. In the same way, we obtain

$$\begin{aligned} \ln \Lambda^{\max}(v) &= \Psi_N(v) + \zeta * \ln \mathfrak{A}_0(v) + \overline{\zeta} * \ln \overline{\mathfrak{A}}_0(v) + (\zeta + \overline{\zeta}) * \ln \mathfrak{A}_1(v) \\ \Psi_N(v) &= \frac{N}{2} \ln \frac{\mathrm{sh}(\mathrm{i}v + u_N + \gamma(\alpha+1))\mathrm{sh}(\mathrm{i}v - u_N - \gamma(\alpha+1))}{\mathrm{sh}(\mathrm{i}v - u_N + \gamma(\alpha+1))\mathrm{sh}(\mathrm{i}v + u_N - \gamma(\alpha+1))}. \end{aligned} \tag{B.13}$$

In these NLIEs, we can take the Trotter limit $N \to \infty$ analytically:

$$\lim_{N\to\infty} \psi_N(v) = \psi(v) \qquad \lim_{N\to\infty} \Psi_N(v) = \Psi(v). \tag{B.14}$$

We have determined the integration constants $\beta\mu$, $2\beta\mu$ in (3.2) and 0 in (3.5) by taking the limit $|\mathrm{i}v| \to \infty$ (note that we take this limit by making use of analytic continuation of the NLIEs (see appendix D)) and comparing the results with

$$\mathfrak{a}_0 \to \frac{\mathrm{e}^{\beta\mu}}{\mathrm{e}^{\beta\mu}+1} \qquad \overline{\mathfrak{a}}_0 \to \frac{\mathrm{e}^{\beta\mu}}{\mathrm{e}^{\beta\mu}+1} \qquad \mathfrak{a}_1 \to \frac{\mathrm{e}^{2\beta\mu}}{2\mathrm{e}^{\beta\mu}+1} \qquad \Lambda \to (\mathrm{e}^{\beta\mu}+1)^2. \tag{B.15}$$

Appendix C. Derivation of NLIEs for excited states

Here we consider the excited states characterizing the correlations which are discussed in the main text. As mentioned in section 3, the excited states are described by certain distribution patterns of additional zeros and poles which enter the physical strip. To derive the NLIEs, we must explore these zeros and poles. By taking the integration contours in a way that they circumvent the zeros in the physical strip, we can derive the NLIEs directly by utilizing the above results for the largest eigenvalue.

Taking the integration contours of the convolutions in (B.12) as in figure C.1 (and subsequent figures), we have the same algebraic structure of NLIEs as in (B.12) without additive terms. This is true at least in the case of the intermediate (differentiated) version of (B.12) where $\ln \mathfrak{a}$, $\ln \mathfrak{A}$, ψ_N are replaced by $(\ln \mathfrak{a})'$, $(\ln \mathfrak{A})'$, ψ_N'.

When integrating the NLIEs with respect to the argument we want to make sure that the convolutions are understood in the manner $k * (\ln \mathfrak{A})'(v) := \int_C k(x)(\ln \mathfrak{A})'(v-x)\,\mathrm{d}x$ with a v-independent path C. This can always be achieved with C starting (ending) at $-\pi/2$ ($+\pi/2$) and suitable deformations in order to avoid the singularities. The integration with respect to v and up to an integration constant yields a set of NLIEs which has the same algebraic structure as in the case of the largest eigenvalue where now terms $k * \ln \mathfrak{A}(v) = \int_C k(x) \ln \mathfrak{A}(v-x)\,\mathrm{d}x$ appear

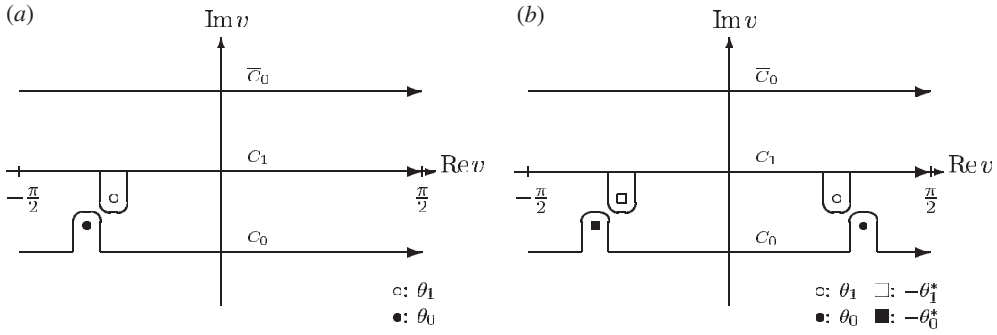

Figure C.1. Integration contours for (*a*) the one-particle Green function and (*b*) the triplet superconducting pair correlations. Here C_0, $\overline{C}_0$ and C_1 denote the contours for $\mathfrak{A}_0$, $\overline{\mathfrak{A}}_0$ and $\mathfrak{A}_1$, respectively.

with deformed contours. Alternatively, we can straighten the contours and due to Cauchy's theorem obtain additional terms from the singularities of the auxiliary functions (these are the 'sin' terms below).

On top of these terms we obtain a second set of additional terms. Note that the functions $\ln \mathfrak{A}_0(v)$ and $\ln \mathfrak{A}_1(v)$ are not periodic: $\ln \mathfrak{A}_0(\pi/2) - \ln \mathfrak{A}_0(-\pi/2) = 2\pi\mathrm{i}$ and $\ln \mathfrak{A}_1(\pi/2) - \ln \mathfrak{A}_1(-\pi/2) = 2\pi\mathrm{i}$ for the one-particle Green functions and $\ln \mathfrak{A}_0(\pi/2) - \ln \mathfrak{A}_0(-\pi/2) = 4\pi\mathrm{i}$ and $\ln \mathfrak{A}_1(\pi/2) - \ln \mathfrak{A}_1(-\pi/2) = 4\pi\mathrm{i}$ for the triplet superconducting pair correlations. Further note that $k * \ln \mathfrak{A}(v) = \int_C k(x) \ln \mathfrak{A}(v-x)\,\mathrm{d}x = \int_{v-C} k(v-x) \ln \mathfrak{A}(x)\,\mathrm{d}x$ which in the general case (non-periodic $\ln \mathfrak{A}$) is different from $\int_{-C} k(v-x) \ln \mathfrak{A}(x)\,\mathrm{d}x$. For many numerical applications we actually like to have convolutions of the last type where the auxiliary functions are evaluated on fixed (straight) contours. The difference of the two versions of convolution integrals can be worked out and gives rise to the 'cos' terms below.

By use of the analytic continuation of the NLIE (see appendix D), one determines the integration constants in a manner similar to the largest eigenvalue case.

We want to categorize the additional zeros and poles of the auxiliary functions in the following four cases of excitations: (1) the one-particle Green functions and the triplet superconducting pair correlations, (2) the density–density (longitudinal) correlations, (3) the transversal spin–spin correlations and (4) the singlet superconducting pair correlations.

C.1. One-particle Green function and triplet superconducting pair correlations

First we consider the NLIE for the one-particle Green functions $\langle c^\dagger_{j,\sigma} c_{i,\sigma} \rangle$. In this case, the eigenvalues (2.31) belong to the sector $n = N - 1$ and $m = N/2 - 1$. From the numerical calculations with finite Trotter number N, we observe additional zeros, namely a zero θ_0 of the auxiliary function $\mathfrak{A}_0(v)$ and a zero θ_1 of $\mathfrak{A}_1(v)$ located in the lower half-plane. The zeros θ_0 and θ_1 are derived from

$$\lambda_2\left(\theta_0 + \frac{\mathrm{i}}{2}\gamma\alpha\right) + \lambda_3\left(\theta_0 + \frac{\mathrm{i}}{2}\gamma\alpha\right) + \lambda_4\left(\theta_0 + \frac{\mathrm{i}}{2}\gamma\alpha\right) = 0 \qquad q_1^h\left(\theta_1 + \frac{\mathrm{i}}{2}\gamma\alpha\right) = 0. \quad \text{(C.1)}$$

In the case for the triplet superconducting pair correlations $\langle c^\dagger_{j+1,\uparrow} c^\dagger_{j,\uparrow} c_{i+1,\downarrow} c_{i,\downarrow} \rangle$, the corresponding eigenvalues (2.31) describing these correlations belong to the sector $n = N - 2$ and $m = N/2 - 2$. Numerically we observe additional parameters: zeros θ_0, $-\theta_0^*$ for the function $\mathfrak{A}_0(v)$ and zeros θ_1, $-\theta_1^*$ for function $\mathfrak{A}_1(v)$ appear in the lower half-plane (the

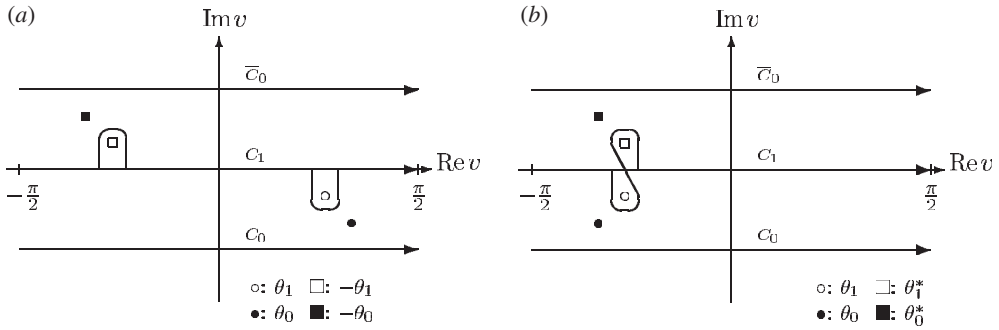

Figure C.2. Integration contours of the NLIE for (*a*) the dominant and (*b*) sub-dominant contributions to the density–density correlations.

symbol $*$ denotes complex conjugation). As for the one-particle Green function, the zeros θ_0 ($-\theta_0^*$) and θ_1 (θ_1^*) satisfy the first and the second equation in (C.1), respectively.

C.2. Density–density correlations

Let us consider the NLIEs for the density–density correlations $\langle n_j n_i \rangle$. The eigenvalues (2.31) belong to the sector $n = N$ and $m = N/2$ which is the same sector as for the largest eigenvalue. These correlations are described by the distribution patterns of a zero θ_0 ($-\theta_0$) and a pole θ_1 ($-\theta_1$) of the auxiliary function $\mathfrak{A}_0(v)$ ($\overline{\mathfrak{A}}_0(v)$) appearing in the physical strip. In this case, these zeros and poles are derived from

$$\begin{aligned} &q_2^h\left(\theta_0 + \frac{\mathrm{i}}{2}\gamma\alpha\right) = 0 \qquad q_2\left(-\theta_0 + \frac{\mathrm{i}}{2}\gamma\alpha\right) = 0 \\ &q_1^h\left(\theta_1 + \frac{\mathrm{i}}{2}\gamma\alpha\right) = 0 \qquad q_1\left(-\theta_1 + \frac{\mathrm{i}}{2}\gamma(\alpha+1)\right) = 0. \end{aligned} \tag{C.2}$$

In addition, we can consider the sub-dominant terms described by simple particle–hole excitations at each Fermi point (see section 4). These sub-dominant terms are determined from zeros θ_0 (θ_0^*) for $\mathfrak{A}_0(v)$ ($\overline{\mathfrak{A}}_0(v)$) and θ_1, θ_1^* for $\mathfrak{A}_1(v)$, respectively. These zeros and poles satisfy equation (C.2) (replace $-\theta_1$ and $-\theta_0$ by $-\theta_1 \to \theta_1^*$ and $-\theta_0 \to \theta_0^*$, respectively). Taking the integration contours as in figure C.2, we arrive at NLIEs which have the same form as in (B.12). For both cases, we take the convolutions in the ordinary way, i.e. as for the largest eigenvalue.

C.3. Transversal spin–spin correlations

Let us consider the eigenvalues which describe the transversal spin–spin correlations $\langle \sigma_j^+ \sigma_i^- \rangle$. The eigenvalues (2.31) belong to the sector $n = N$ and $m = N/2 - 1$. Making use of numerical calculations, we observe that additional zeros θ_0 ($-\theta_0$) and poles θ_1 ($-\theta_1$) of the auxiliary function $\mathfrak{A}_0(v)$ ($\overline{\mathfrak{A}}_0(v)$) appear in the lower (upper) half-plane. As in case (1), these zeros and poles get close to but never cross the real axis in the low-temperature limit. These additional zeros (poles) are derived from

$$\begin{aligned} &\lambda_2\left(\pm\theta_0 + \frac{\mathrm{i}}{2}\gamma\alpha\right) + \lambda_3\left(\pm\theta_0 + \frac{\mathrm{i}}{2}\gamma\alpha\right) + \lambda_4\left(\pm\theta_0 + \frac{\mathrm{i}}{2}\gamma\alpha\right) = 0 \\ &q_1^h\left(\theta_1 + \frac{\mathrm{i}}{2}\gamma\alpha\right) = 0 \qquad q_1\left(-\theta_1 + \frac{\mathrm{i}}{2}\gamma(\alpha+1)\right) = 0. \end{aligned} \tag{C.3}$$

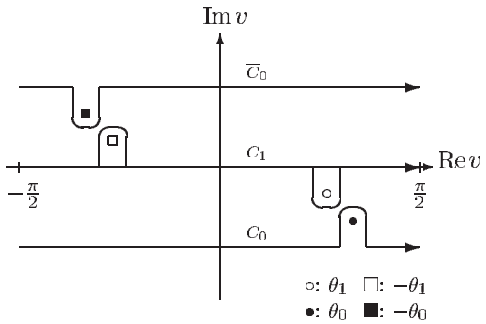

Figure C.3. Integration contours of the NLIE for the transversal spin–spin correlations.

We derive the NLIEs by taking the contours as in figure C.3.

C.4. Singlet superconducting pair correlations

We consider the singlet superconducting pair correlations $\langle c^\dagger_{j+1,\uparrow} c^\dagger_{j,\downarrow} c_{i+1,\uparrow} c_{i,\downarrow}\rangle$. In this case, the eigenvalues written as (2.31) belong to the sector $n = N - 2$ and $m = N/2 - 1$. These correlations are described by the distribution patterns of zeros θ_0, $\overline{\theta}_0$, $\tilde{\theta}_0$ and poles θ_1, $-\theta_1^*$ of the auxiliary function $\mathfrak{A}_0(v)$. Numerically we observe that the zero $\tilde{\theta}_0$ is located on the $\pm\pi/2$-axis ($\mathrm{Re}\, v = \pm\pi/2$) and moves to the real axis with decreasing temperature. At sufficiently high temperatures, the zeros θ_0 and $\overline{\theta}_0$ are related by $\overline{\theta}_0 = -\theta_0^*$ and get close to the boundary ($\pm\pi/2$-axis) with decreasing temperature. At a certain temperature T_c, the zeros θ_0, $\overline{\theta}_0$ and θ_0^* satisfy $\theta_0 = \overline{\theta}_0 = \theta_0^*$. Below T_c, the relation $\overline{\theta}_0 = -\theta_0^*$ is no longer valid, and these zeros are located on the $\pi/2$-axis satisfying the relation $\mathrm{Im}\,\overline{\theta}_0 < \mathrm{Im}\,\tilde{\theta}_0 < \mathrm{Im}\,\theta_0$. $\tilde{\theta}_0$ and θ_0 move upwards (in the +i direction along the $\pi/2$-axis), opposite to this $\overline{\theta}_0$ moves in the $-$i direction. In the low-temperature limit, $\tilde{\theta}_0$ comes near to the real axis but never crosses it. On the other hand θ_0 enters the upper half-plane and finally leaves the physical strip. $\overline{\theta}_0$ also leaves the physical strip in the lower half-plane. Consequently, at low temperature, only θ_1 and $-\theta_1^*$ (zeros of $\mathfrak{A}_1(v)$) are circumvented by the integration contour of $\mathfrak{A}_1(v)$ and these zeros characterize the massless pair-excitations (see section 4).

Due to this behaviour, we must take different integration contours for the different regimes $T > T_c$ and $T < T_c$. These zeros are derived from

$$\begin{aligned}
&\lambda_2\left(\theta_0 + \frac{\mathrm{i}}{2}\gamma\alpha\right) + \lambda_3\left(\theta_0 + \frac{\mathrm{i}}{2}\gamma\alpha\right) + \lambda_4\left(\theta_0 + \frac{\mathrm{i}}{2}\gamma\alpha\right) = 0 \\
&\lambda_2\left(\overline{\theta}_0 + \frac{\mathrm{i}}{2}\gamma\alpha\right) + \lambda_3\left(\overline{\theta}_0 + \frac{\mathrm{i}}{2}\gamma\alpha\right) + \lambda_4\left(\overline{\theta}_0 + \frac{\mathrm{i}}{2}\gamma\alpha\right) = 0 \qquad \text{(C.4)} \\
&q_2^h(\tilde{\theta}_0) = 0 \qquad q_1^h\left(\theta_1 + \frac{\mathrm{i}}{2}\gamma\alpha\right) = 0 \qquad q_1\left(-\theta_1 + \frac{\mathrm{i}}{2}\gamma(\alpha+1)\right) = 0.
\end{aligned}$$

We derive the NLIEs by taking the integration contours as in figure C.4(a) for the case $T > T_c$ and as in figure C.4(b) for the case $T < T_c$.

C.4.1. Additional terms in the NLIEs. As mentioned above, we obtain the same structure of NLIEs as in the case of the largest eigenvalue by taking the integration contours of the convolutions in such a way that they circumvent the zeros. To solve the NLIEs numerically, we are forced to use straight integration contours. Due to Cauchy's theorem in this formulation we

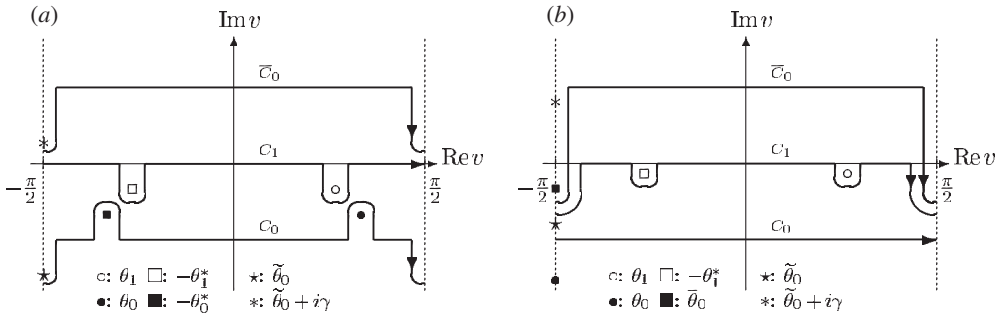

Figure C.4. Integration contours of the NLIE for the singlet superconducting pair correlations for (*a*) $T > T_c$ and (*b*) $T < T_c$.

obtain certain additional terms in the NLIEs. In what follows we list the additional contributions to the driving terms in (3.7) and (3.8).

One-particle Green function. First we consider the one-particle Green function. The corresponding NLIEs are characterized by the zeros θ_0 and θ_1. In the low-temperature limit, these parameters come near to the real axis but never enter the upper half-plane. From (C.1), we find that these parameters satisfy the subsidiary conditions

$$\begin{aligned} &\mathfrak{A}_0(\theta_0) = \overline{\mathfrak{A}}_0(\theta_0) = 0 \qquad \mathfrak{A}_0(\theta_1) = \infty \\ &\mathfrak{A}_1(\theta_1) = 0 \qquad \mathfrak{A}_1(\theta_0) = \infty. \end{aligned} \tag{C.5}$$

Performing the Fourier transform and employing Cauchy's theorem, we determine the NLIE (3.7) with the following additional terms:

$$\begin{aligned} \overline{\varphi}_0^{(0)}(v) &= \begin{cases} \dfrac{\cos(v - \mathrm{i}\gamma + \mathrm{i}\delta)}{\cos(v + \mathrm{i}\delta)} & \text{for} \quad \operatorname{Im}\theta_0 < -\delta \\ \dfrac{\sin(v - \theta_0 - \mathrm{i}\gamma)}{\sin(v - \theta_0)} & \text{for} \quad -\delta < \operatorname{Im}\theta_0 < 0 \end{cases} \\ \overline{\varphi}_0^{(1)}(v) &= \begin{cases} \dfrac{\cos(v + \mathrm{i}\delta)}{\cos(v - \mathrm{i}\gamma + \mathrm{i}\delta)} & \text{for} \quad \operatorname{Im}\theta_1 < -\delta \\ \dfrac{\sin(v - \theta_1)}{\sin(v - \theta_1 - \mathrm{i}\gamma)} & \text{for} \quad -\delta < \operatorname{Im}\theta_1 < 0 \end{cases} \\ \overline{\varphi}_0(v) &= \overline{\varphi}_0^{(0)}(v)\overline{\varphi}_0^{(1)}(v) \qquad \varphi_0(v) = \frac{\sin(v - \theta_1 + \mathrm{i}\gamma)}{\sin(v - \theta_1)} \\ \varphi_1(v) &= \varphi_0(v)\overline{\varphi}_0(v). \end{aligned} \tag{C.6}$$

The corresponding eigenvalues $\Lambda(v)$ are written as (3.8) with the term $\chi(v)$ (split into two terms $\chi(v) = \chi^{(0)}(v)\chi^{(1)}(v)$),

$$\chi(v) = \chi^{(0)}(v)\chi^{(1)}(v)$$

$$\chi^{(0)}(v) = \begin{cases} \dfrac{\cos(v + \frac{\mathrm{i}}{2}\gamma\alpha + \mathrm{i}\delta)}{\cos(v - \frac{\mathrm{i}}{2}\gamma(\alpha+2) + \mathrm{i}\delta)} & \text{for} \quad \operatorname{Im}\theta_0 < -\delta \\ \dfrac{\sin(v - \theta_0 + \frac{\mathrm{i}}{2}\gamma\alpha)}{\sin(v - \theta_0 - \frac{\mathrm{i}}{2}\gamma(\alpha+2))} & \text{for} \quad -\delta < \operatorname{Im}\theta_0 < 0 \end{cases}$$

$$\chi^{(1)}(v) = \frac{\sin(v-\theta_1-\frac{\mathrm{i}}{2}\alpha\gamma)}{\sin(v-\theta_1+\frac{\mathrm{i}}{2}\gamma(\alpha+2))} \times \begin{cases} \dfrac{\cos(v-\frac{\mathrm{i}}{2}\gamma(\alpha+2)+\mathrm{i}\delta)}{\cos(v+\frac{\mathrm{i}}{2}\gamma\alpha+\mathrm{i}\delta)} & \text{for} \quad \operatorname{Im}\theta_1 < -\delta \\ \dfrac{\sin(v-\theta_1-\frac{\mathrm{i}}{2}\gamma(\alpha+2))}{\sin(v-\theta_1+\frac{\mathrm{i}}{2}\alpha\gamma)} & \text{for} \quad -\delta < \operatorname{Im}\theta_1 < 0. \end{cases} \tag{C.7}$$

In fact the NLIE (3.7) with the additional terms (C.6) have two solutions. These two solutions are related to each other by taking the mirror image with respect to the imaginary axis. Correspondingly, the eigenvalues $\Lambda(0)$ are doubly degenerate in magnitude and they are complex conjugate to each other. The oscillatory behaviour of the one-particle Green function (referred to as k_{F} oscillation at zero temperature) derives from this degeneracy. The correlation length for the one-particle Green function is given through formula (2.29).

Triplet superconducting pair correlations. We determine the additional terms for the triplet superconducting pair correlations. As mentioned above, these correlations are characterized by the additional zeros θ_0 and θ_1. In the low-temperature limit, these zeros come near the real axis but never enter the upper half-plane. From (C.1), one finds that these zeros satisfy

$$\begin{aligned} &\mathfrak{A}_0(\theta_0) = \mathfrak{A}_0(-\theta_0^*) = \overline{\mathfrak{A}}_0(\theta_0) = \overline{\mathfrak{A}}_0(-\theta_0^*) = 0 \qquad \mathfrak{A}_0(\theta_1) = \mathfrak{A}_0(-\theta_1^*) = \infty \\ &\mathfrak{A}_1(\theta_1) = \mathfrak{A}_1(-\theta_1^*) = 0 \qquad \mathfrak{A}_1(\theta_0) = \mathfrak{A}_1(-\theta_0^*) = \infty. \end{aligned} \tag{C.8}$$

Performing the Fourier transform and employing Cauchy's theorem, we determine the NLIE (3.7) with the following additional terms:

$$\overline{\varphi}_0^{(0)}(v) = \begin{cases} \dfrac{\cos^2(v-\mathrm{i}\gamma+\mathrm{i}\delta)}{\cos^2(v+\mathrm{i}\delta)} & \text{for} \quad \operatorname{Im}\theta_0 < -\delta \\ \dfrac{\sin(v-\theta_0-\mathrm{i}\gamma)\sin(v+\theta_0^*-\mathrm{i}\gamma)}{\sin(v-\theta_0)\sin(v+\theta_0^*)} & \text{for} \quad -\delta < \operatorname{Im}\theta_0 < 0 \end{cases}$$

$$\overline{\varphi}_0^{(1)}(v) = \begin{cases} \dfrac{\cos^2(v+\mathrm{i}\delta)}{\cos^2(v-\mathrm{i}\gamma+\mathrm{i}\delta)} & \text{for} \quad \operatorname{Im}\theta_1 < -\delta \\ \dfrac{\sin(v-\theta_1)\sin(v+\theta_1^*)}{\sin(v-\theta_1-\mathrm{i}\gamma)\sin(v+\theta_1^*-\mathrm{i}\gamma)} & \text{for} \quad -\delta < \operatorname{Im}\theta_1 < 0 \end{cases} \tag{C.9}$$

$$\overline{\varphi}_0(v) = \overline{\varphi}_0^{(0)}(v)\overline{\varphi}_0^{(1)}(v) \qquad \varphi_0(v) = \frac{\sin(v-\theta_1+\mathrm{i}\gamma)\sin(v+\theta_1^*+\mathrm{i}\gamma)}{\sin(v-\theta_1)\sin(v+\theta_1^*)}$$

$$\varphi_1(v) = \varphi_0(v)\overline{\varphi}_0(v).$$

The corresponding eigenvalues $\Lambda(v)$ are written as (3.8) with the term $\chi(v)$,

$$\chi(v) = \chi^{(0)}(v)\chi^{(1)}(v)$$

$$\chi^{(0)}(v) = \begin{cases} \dfrac{\cos^2(v+\frac{\mathrm{i}}{2}\gamma\alpha+\mathrm{i}\delta)}{\cos^2(v-\frac{\mathrm{i}}{2}\gamma(\alpha+2)+\mathrm{i}\delta)} & \text{for} \quad \operatorname{Im}\theta_0 < -\delta \\ \dfrac{\sin(v-\theta_0+\frac{\mathrm{i}}{2}\gamma\alpha)\sin(v+\theta_0^*+\frac{\mathrm{i}}{2}\gamma\alpha)}{\sin(v-\theta_0-\frac{\mathrm{i}}{2}\gamma(\alpha+2))\sin(v+\theta_0^*-\frac{\mathrm{i}}{2}\gamma(\alpha+2))} & \text{for} \quad -\delta < \operatorname{Im}\theta_0 < 0 \end{cases} \tag{C.10}$$

$$\chi^{(1)}(v) = \frac{\sin(v-\theta_1-\frac{\mathrm{i}}{2}\alpha\gamma)\sin(v+\theta_1^*-\frac{\mathrm{i}}{2}\alpha\gamma)}{\sin(v-\theta_1+\frac{\mathrm{i}}{2}\gamma(\alpha+2))\sin(v+\theta_1^*+\frac{\mathrm{i}}{2}\gamma(\alpha+2))}$$
$$\times\begin{cases}\dfrac{\cos^2(v-\frac{\mathrm{i}}{2}\gamma(\alpha+2)+\mathrm{i}\delta)}{\cos^2(v+\frac{\mathrm{i}}{2}\gamma\alpha+\mathrm{i}\delta)} & \text{for}\quad \operatorname{Im}\theta_1<-\delta\\ \dfrac{\sin(v-\theta_1-\frac{\mathrm{i}}{2}\gamma(\alpha+2))\sin(v+\theta_1^*-\frac{\mathrm{i}}{2}\gamma(\alpha+2))}{\sin(v-\theta_1+\frac{\mathrm{i}}{2}\alpha\gamma)\sin(v+\theta_1^*+\frac{\mathrm{i}}{2}\alpha\gamma)} & \text{for}\quad -\delta<\operatorname{Im}\theta_1<0.\end{cases} \tag{C.11}$$

Density–density (longitudinal spin–spin) correlations. Next we determine the NLIE for the density–density correlations. As the critical exponents of the density–density correlation functions are identical to those of the longitudinal spin–spin correlations $\langle\sigma_j^z\sigma_i^z\rangle$, the resultant NLIEs are also identical. From (C.2), we find these zeros satisfy the subsidiary conditions

$$\mathfrak{A}_0(\theta_0)=\overline{\mathfrak{A}}_0(-\theta_0)=0 \qquad \mathfrak{A}_0(\theta_1)=\overline{\mathfrak{A}}_0(-\theta_1)=\infty \qquad \mathfrak{A}_1(\pm\theta_1)=0. \tag{C.12}$$

Correspondingly, the additional terms in the NLIE (3.7) read

$$\overline{\varphi}_0^{(0)}(v)=\begin{cases}\dfrac{\sin(v-\theta_0)\cos(v-\mathrm{i}\gamma+\mathrm{i}\delta)}{\sin(v-\theta_0-\mathrm{i}\gamma)\cos(v+\mathrm{i}\delta)} & \text{for}\quad \operatorname{Im}\theta_0<-\delta\\ 1 & \text{for}\quad -\delta<\operatorname{Im}\theta_0\end{cases}$$
$$\overline{\varphi}_0^{(1)}(v)=\frac{\sin(v+\theta_1-\mathrm{i}\gamma)}{\sin(v+\theta_1)}\times\begin{cases}\dfrac{\cos(v+\mathrm{i}\delta)}{\cos(v-\mathrm{i}\gamma+\mathrm{i}\delta)} & \text{for}\quad \operatorname{Im}\theta_1<-\delta\\ \dfrac{\sin(v-\theta_1)}{\sin(v-\theta_1-\mathrm{i}\gamma)} & \text{for}\quad -\delta<\operatorname{Im}\theta_1<0\end{cases} \tag{C.13}$$
$$\overline{\varphi}_0(v)=\overline{\varphi}_0^{(0)}(v)\overline{\varphi}_0^{(1)}(v) \qquad \varphi_0(v)=\overline{\varphi}_0(-v) \qquad \varphi_1(v)=\varphi_0(v)\overline{\varphi}_0(v).$$

The additional term $\chi(v)$ in (3.8) is determined from

$$\chi(v)=\chi^{(0)}(v)\chi^{(1)}(v)$$
$$\chi^{(0)}(v)=\begin{cases}\dfrac{\sin(v-\theta_0-\frac{\mathrm{i}}{2}\gamma(\alpha+2))\sin(v+\theta_0+\frac{\mathrm{i}}{2}\gamma(\alpha+2))\cos(v+\frac{\mathrm{i}}{2}\gamma\alpha+\mathrm{i}\delta)\cos(v-\frac{\mathrm{i}}{2}\gamma\alpha-\mathrm{i}\delta)}{\sin(v-\theta_0+\frac{\mathrm{i}}{2}\gamma\alpha)\sin(v+\theta_0-\frac{\mathrm{i}}{2}\gamma\alpha)\cos(v-\frac{\mathrm{i}}{2}\gamma(\alpha+2)+\mathrm{i}\delta)\cos(v+\frac{\mathrm{i}}{2}\gamma(\alpha+2)-\mathrm{i}\delta)}\\ \text{for}\quad \operatorname{Im}\theta_0<-\delta\\ 1\\ \text{for}\quad -\delta<\operatorname{Im}\theta_0\end{cases}$$
$$\chi^{(1)}(v)=\frac{\sin(v-\theta_1-\frac{\mathrm{i}}{2}\alpha\gamma)\sin(v+\theta_1+\frac{\mathrm{i}}{2}\alpha\gamma)}{\sin(v-\theta_1+\frac{\mathrm{i}}{2}\gamma(\alpha+2))\sin(v+\theta_1-\frac{\mathrm{i}}{2}\gamma(\alpha+2))}$$
$$\times\begin{cases}\dfrac{\cos(v-\frac{\mathrm{i}}{2}\gamma(\alpha+2)+\mathrm{i}\delta)\cos(v+\frac{\mathrm{i}}{2}\gamma(\alpha+2)-\mathrm{i}\delta)}{\cos(v+\frac{\mathrm{i}}{2}\gamma\alpha+\mathrm{i}\delta)\cos(v-\frac{\mathrm{i}}{2}\gamma\alpha-\mathrm{i}\delta)} & \text{for}\quad \operatorname{Im}\theta_1<-\delta\\ \dfrac{\sin(v-\theta_1-\frac{\mathrm{i}}{2}\gamma(\alpha+2))\sin(v+\theta_1+\frac{\mathrm{i}}{2}\gamma(\alpha+2))}{\sin(v-\theta_1+\frac{\mathrm{i}}{2}\alpha\gamma)\sin(v+\theta_1-\frac{\mathrm{i}}{2}\alpha\gamma)} & \text{for}\quad -\delta<\operatorname{Im}\theta_1<0.\end{cases} \tag{C.14}$$

In the low-temperature limit, θ_1 gets close to the real axis but does not cross it. In contrast, θ_0 crosses the real axis and enters the upper half-plane. Hence only one additional zero θ_1 appears explicitly in the above NLIE, which is characteristic of massless excitations (see section 4). The solutions to the above NLIE have the symmetry $\overline{\mathfrak{a}}_0(v)=\mathfrak{a}_0(-v)$ and $\mathfrak{a}_1(v)$ is symmetric with respect to the imaginary axis. The NLIEs (C.13) have two solutions which are connected with each other by taking the mirror image with respect to the imaginary axis. Hence the corresponding eigenvalues $\Lambda(0)$ are degenerate in magnitude; they are complex

conjugate to each other. Due to this degeneracy, the correlations have an oscillation factor. At zero temperature, this oscillatory behaviour is the characteristic $2k_F$ oscillation in the density–density correlations.

The sub-dominant terms discussed above are characterized by another distribution pattern of zeros and poles. Consequently, a zero θ_0 (θ_0^*) and a pole θ_1 (θ_1^*) of the functions $\mathfrak{a}_0(v)$ ($\overline{\mathfrak{a}}_0(v)$) appear in the physical strip. From (C.2) (replace $-\theta_1$ and $-\theta_0$ by $-\theta_1 \to \theta_1^*$ and $-\theta_0 \to \theta_0^*$, respectively), we find that these zeros and poles satisfy the subsidiary conditions

$$\mathfrak{A}_0(\theta_0) = \overline{\mathfrak{A}}_0(\theta_0^*) = 0 \qquad \mathfrak{A}_0(\theta_1) = \overline{\mathfrak{A}}_0(\theta_1^*) = \infty \qquad \mathfrak{A}_1(\theta_1) = \mathfrak{A}_1(\theta_1^*) = 0. \tag{C.15}$$

In the same way as before one obtains the NLIEs characterized by the following additional terms:

$$\begin{aligned}
\overline{\varphi}_0^{(0)}(v) &= \begin{cases} \dfrac{\sin(v-\theta_0)\cos(v-\mathrm{i}\gamma+\mathrm{i}\delta)}{\sin(v-\theta_0-\mathrm{i}\gamma)\cos(v+\mathrm{i}\delta)} & \text{for} \quad \operatorname{Im}\theta_0 < -\delta \\ 1 & \text{for} \quad -\delta < \operatorname{Im}\theta_0 \end{cases} \\
\overline{\varphi}_0^{(1)}(v) &= \frac{\sin(v-\theta_1^*-\mathrm{i}\gamma)}{\sin(v-\theta_1^*)} \times \begin{cases} \dfrac{\cos(v+\mathrm{i}\delta)}{\cos(v-\mathrm{i}\gamma+\mathrm{i}\delta)} & \text{for} \quad \operatorname{Im}\theta_1 < -\delta \\ \dfrac{\sin(v-\theta_1)}{\sin(v-\theta_1-\mathrm{i}\gamma)} & \text{for} \quad -\delta < \operatorname{Im}\theta_1 < 0 \end{cases} \\
\overline{\varphi}_0(v) &= \overline{\varphi}_0^{(0)}(v)\overline{\varphi}_0^{(1)}(v) \qquad \varphi_0(v) = \overline{\varphi}_0^*(v) \qquad \varphi_1(v) = \varphi_0(v)\overline{\varphi}_0(v).
\end{aligned} \tag{C.16}$$

The term $\chi(v)$ in the eigenvalues (3.8) is written as

$$\begin{aligned}
\chi(v) &= \chi^{(0)}(v)\chi^{(1)}(v) \\
\chi^{(0)}(v) &= \begin{cases} \dfrac{\sin(v-\theta_0-\frac{\mathrm{i}}{2}\gamma(\alpha+2))\sin(v-\theta_0^*+\frac{\mathrm{i}}{2}\gamma(\alpha+2))\cos(v+\frac{\mathrm{i}}{2}\gamma\alpha+\mathrm{i}\delta)\cos(v-\frac{\mathrm{i}}{2}\gamma\alpha-\mathrm{i}\delta)}{\sin(v-\theta_0+\frac{\mathrm{i}}{2}\gamma\alpha)\sin(v-\theta_0^*-\frac{\mathrm{i}}{2}\gamma\alpha)\cos(v-\frac{\mathrm{i}}{2}\gamma(\alpha+2)+\mathrm{i}\delta)\cos(v+\frac{\mathrm{i}}{2}\gamma(\alpha+2)-\mathrm{i}\delta)} \\ \text{for} \quad \operatorname{Im}\theta_0 < -\delta \\ 1 \\ \text{for} \quad -\delta < \operatorname{Im}\theta_0 \end{cases} \\
\chi^{(1)}(v) &= \frac{\sin(v-\theta_1-\frac{\mathrm{i}}{2}\alpha\gamma)\sin(v-\theta_1^*+\frac{\mathrm{i}}{2}\alpha\gamma)}{\sin(v-\theta_1+\frac{\mathrm{i}}{2}\gamma(\alpha+2))\sin(v-\theta_1^*-\frac{\mathrm{i}}{2}\gamma(\alpha+2))} \\
&\times \begin{cases} \dfrac{\cos(v-\frac{\mathrm{i}}{2}\gamma(\alpha+2)+\mathrm{i}\delta)\cos(v+\frac{\mathrm{i}}{2}\gamma(\alpha+2)-\mathrm{i}\delta)}{\cos(v+\frac{\mathrm{i}}{2}\gamma\alpha+\mathrm{i}\delta)\cos(v-\frac{\mathrm{i}}{2}\gamma\alpha-\mathrm{i}\delta)} & \text{for} \quad \operatorname{Im}\theta_1 < -\delta \\ \dfrac{\sin(v-\theta_1-\frac{\mathrm{i}}{2}\gamma(\alpha+2))\sin(v-\theta_1^*+\frac{\mathrm{i}}{2}\gamma(\alpha+2))}{\sin(v-\theta_1+\frac{\mathrm{i}}{2}\alpha\gamma)\sin(v-\theta_1^*-\frac{\mathrm{i}}{2}\alpha\gamma)} & \text{for} \quad -\delta < \operatorname{Im}\theta_1 < 0. \end{cases}
\end{aligned} \tag{C.17}$$

At low temperatures, the parameter θ_1 (zero of the function $\mathfrak{A}_1(v)$) moves toward the real axis but never crosses it, whereas θ_0 (zero of the function $\mathfrak{A}_0(v)$) crosses the real axis and enters the upper half-plane. In this limit, the NLIEs depend only on the two zeros (of $\mathfrak{A}_1(v)$) θ_1 and θ_1^*, which characterize the particle–hole excitations (see section 4).

Note that the solutions to the above NLIEs satisfy $\mathfrak{a}_0^*(v) = \overline{\mathfrak{a}}_0(v)$ and $\mathfrak{a}_1(v)$ is symmetric with respect to the real axis but not to the imaginary axis. Therefore $\mathfrak{a}_1(v)$ is real for $v \in \mathbb{R}$. The three NLIE are also reducible as in the dominant case. The NLIE with (C.16) admits two solutions. In contrast to the above dominant case, they are related to each other by taking the mirror image with respect to the real axis. The corresponding eigenvalues $\Lambda(0)$ are degenerate and are real. Hence one finds that the corresponding correlations do not have oscillatory terms.

Transversal spin–spin correlations. Let us determine the additional terms of the NLIEs describing the transversal spin–spin correlations. As mentioned above, these correlations are characterized by the zeros and poles satisfying equation (C.3). Hence we find that these zeros (poles) satisfy the following subsidiary conditions:

$$\begin{aligned} &\mathfrak{A}_0(\pm\theta_0) = \overline{\mathfrak{A}}_0(\pm\theta_0) = 0 \qquad \mathfrak{A}_0(\theta_1) = \overline{\mathfrak{A}}_0(-\theta_1) = \infty \\ &\mathfrak{A}_1(\pm\theta_1) = 0 \qquad \mathfrak{A}_1(\pm\theta_0) = \infty. \end{aligned} \tag{C.18}$$

Consequently, the additional terms are written as follows:

$$\begin{aligned} \overline{\varphi}_0^{(0)}(v) &= \begin{cases} \dfrac{\cos(v - \mathrm{i}\gamma + \mathrm{i}\delta)}{\cos(v + \mathrm{i}\delta)} & \text{for} \quad \operatorname{Im}\theta_0 < -\delta \\ \dfrac{\sin(v - \theta_0 - \mathrm{i}\gamma)}{\sin(v - \theta_0)} & \text{for} \quad -\delta < \operatorname{Im}\theta_0 < 0 \end{cases} \\ \overline{\varphi}_0^{(1)}(v) &= \frac{\sin(v + \theta_1 - \mathrm{i}\gamma)}{\sin(v + \theta_1)} \times \begin{cases} \dfrac{\cos(v + \mathrm{i}\delta)}{\cos(v - \mathrm{i}\gamma + \mathrm{i}\delta)} & \text{for} \quad \operatorname{Im}\theta_1 < -\delta \\ \dfrac{\sin(v - \theta_1)}{\sin(v - \theta_1 - \mathrm{i}\gamma)} & \text{for} \quad -\delta < \operatorname{Im}\theta_1 < 0 \end{cases} \\ \overline{\varphi}_0(v) &= \overline{\varphi}_0^{(0)}(v)\overline{\varphi}_0^{(1)}(v) \qquad \varphi_0(v) = \overline{\varphi}_0(-v) \qquad \varphi_1(v) = \varphi_0(v)\overline{\varphi}_0(v). \end{aligned} \tag{C.19}$$

The term $\chi(v)$ in the eigenvalue (3.8) is written as

$$\begin{aligned} \chi(v) &= \chi^{(0)}(v)\chi^{(1)}(v) \\ \chi^{(0)}(v) &= \begin{cases} \dfrac{\cos(v + \frac{\mathrm{i}}{2}\gamma\alpha + \mathrm{i}\delta)\cos(v - \frac{\mathrm{i}}{2}\gamma\alpha - \mathrm{i}\delta)}{\cos(v - \frac{\mathrm{i}}{2}\gamma(\alpha+2) + \mathrm{i}\delta)\cos(v + \frac{\mathrm{i}}{2}\gamma(\alpha+2) - \mathrm{i}\delta)} & \text{for} \quad \operatorname{Im}\theta_0 < -\delta \\ \dfrac{\sin(v - \theta_0 + \frac{\mathrm{i}}{2}\gamma\alpha)\sin(v + \theta_0 - \frac{\mathrm{i}}{2}\gamma\alpha)}{\sin(v - \theta_0 - \frac{\mathrm{i}}{2}\gamma(\alpha+2))\sin(v + \theta_0 + \frac{\mathrm{i}}{2}\gamma(\alpha+2))} & \text{for} \quad -\delta < \operatorname{Im}\theta_0 < 0 \end{cases} \\ \chi^{(1)}(v) &= \frac{\sin(v - \theta_1 - \frac{\mathrm{i}}{2}\alpha\gamma)\sin(v + \theta_1 + \frac{\mathrm{i}}{2}\alpha\gamma)}{\sin(v - \theta_1 + \frac{\mathrm{i}}{2}\gamma(\alpha+2))\sin(v + \theta_1 - \frac{\mathrm{i}}{2}\gamma(\alpha+2))} \\ &\times \begin{cases} \dfrac{\cos(v - \frac{\mathrm{i}}{2}\gamma(\alpha+2) + \mathrm{i}\delta)\cos(v + \frac{\mathrm{i}}{2}\gamma(\alpha+2) - \mathrm{i}\delta)}{\cos(v + \frac{\mathrm{i}}{2}\gamma\alpha + \mathrm{i}\delta)\cos(v - \frac{\mathrm{i}}{2}\gamma\alpha - \mathrm{i}\delta)} & \text{for} \quad \operatorname{Im}\theta_1 < -\delta \\ \dfrac{\sin(v - \theta_1 - \frac{\mathrm{i}}{2}\gamma(\alpha+2))\sin(v + \theta_1 + \frac{\mathrm{i}}{2}\gamma(\alpha+2))}{\sin(v - \theta_1 + \frac{\mathrm{i}}{2}\alpha\gamma)\sin(v + \theta_1 - \frac{\mathrm{i}}{2}\alpha\gamma)} & \text{for} \quad -\delta < \operatorname{Im}\theta_1 < 0. \end{cases} \end{aligned} \tag{C.20}$$

As in the largest eigenvalue case, the solutions $\mathfrak{a}_0(v)$ and $\overline{\mathfrak{a}}_0(v)$ have the symmetry $\overline{\mathfrak{a}}_0(v) = \mathfrak{a}_0(-v)$. Therefore one reduces the above set of three NLIEs to the set of only two NLIEs. In addition, one finds that the NLIEs (C.19) admit two solutions which are related to each other by taking the mirror image with respect to the imaginary axis. Thus the corresponding eigenvalues $\Lambda(0)$ are degenerate in magnitude and are complex conjugate. Hence, oscillatory behaviour of the correlation functions is observed, referred to as $2k_{\mathrm{F}}$ oscillation for zero temperature.

Singlet superconducting pair correlations. Finally, we consider the NLIE for the singlet superconducting pair correlations characterizing the above-mentioned additional zeros (poles). From (C.4), one sees that these zeros and poles satisfy the subsidiary conditions

$$\begin{aligned} &\mathfrak{A}_0(\theta_0) = \mathfrak{A}_0(\overline{\theta}_0) = \mathfrak{A}_0(\tilde{\theta}_0) = \overline{\mathfrak{A}}_0(\theta_0) = \overline{\mathfrak{A}}_0(\overline{\theta}_0) = 0 \\ &\mathfrak{A}_0(\theta_1) = \mathfrak{A}_0(-\theta_1^*) = \overline{\mathfrak{A}}_0(\theta_1) = \overline{\mathfrak{A}}_0(-\theta_1^*) = \overline{\mathfrak{A}}_0(\tilde{\theta}_0 + \mathrm{i}\gamma) = \infty \\ &\mathfrak{A}_1(\theta_1) = \mathfrak{A}_1(-\theta_1^*) = 0 \qquad \mathfrak{A}_1(\theta_0) = \mathfrak{A}_1(\overline{\theta}_0) = \infty. \end{aligned} \tag{C.21}$$

The additional terms in the NLIE (3.7) read explicitly,

$$\overline{\varphi}_0^{(0)}(v) = \begin{cases} 1 & \text{for} \quad \operatorname{Im}\theta_0 < -\delta \\ \dfrac{\sin(v-\theta_0-\mathrm{i}\gamma)\cos(v+\mathrm{i}\delta)}{\sin(v-\theta_0)\cos(v-\mathrm{i}\gamma+\mathrm{i}\delta)} & \text{for} \quad -\delta < \operatorname{Im}\theta_0 < 0 \\ \dfrac{\cos(v+\mathrm{i}\delta)\cos(v-\mathrm{i}\gamma)}{\cos(v-\mathrm{i}\gamma+\mathrm{i}\delta)\cos(v)} & \text{for} \quad 0 < \operatorname{Im}\theta_0 \end{cases}$$

$$\overline{\varphi}_0^{(\bar{0})}(v) = \begin{cases} 1 & \text{for} \quad \operatorname{Im}\overline{\theta}_0 < -\delta \\ \dfrac{\sin(v-\overline{\theta}_0-\mathrm{i}\gamma)\cos(v+\mathrm{i}\delta)}{\sin(v-\overline{\theta}_0)\cos(v-\mathrm{i}\gamma+\mathrm{i}\delta)} & \text{for} \quad -\delta < \operatorname{Im}\overline{\theta}_0 < 0 \end{cases}$$

$$\overline{\varphi}_0^{(\tilde{0})}(v) = \begin{cases} \dfrac{\sin(v-\tilde{\theta}_0)}{\sin(v-\tilde{\theta}_0-\mathrm{i}\gamma)} & \text{for} \quad \operatorname{Im}\tilde{\theta}_0 < -\delta \\ \dfrac{\cos(v+\mathrm{i}\delta)}{\cos(v-\mathrm{i}\gamma+\mathrm{i}\delta)} & \text{for} \quad -\delta < \operatorname{Im}\tilde{\theta}_0 < 0 \end{cases}$$

$$\overline{\varphi}_0^{(1)}(v) = \begin{cases} 1 & \text{for} \quad \operatorname{Im}\theta_1 < -\delta \\ \dfrac{\sin(v-\theta_1)\sin(v+\theta_1^*)\cos^2(v-\mathrm{i}\gamma+\mathrm{i}\delta)}{\sin(v-\theta_1-\mathrm{i}\gamma)\sin(v+\theta_1^*-\mathrm{i}\gamma)\cos^2(v+\mathrm{i}\delta)} & \text{for} \quad -\delta < \operatorname{Im}\theta_1 < 0 \end{cases} \tag{C.22}$$

$$\varphi_0^{(0)}(v) = \begin{cases} 1 & \text{for} \quad \operatorname{Im}\theta_0 < 0 \\ \dfrac{\sin(v-\theta_0+\mathrm{i}\gamma)\cos(v)}{\sin(v-\theta_0)\cos(v+\mathrm{i}\gamma)} & \text{for} \quad 0 < \operatorname{Im}\theta_0 < \delta \\ \dfrac{\cos(v)\cos(v+\mathrm{i}\gamma-\mathrm{i}\delta)}{\cos(v+\mathrm{i}\gamma)\cos(v-\mathrm{i}\delta)} & \text{for} \quad \delta < \operatorname{Im}\theta_0 \end{cases}$$

$$\varphi_0^{(\tilde{0})}(v) = \begin{cases} \dfrac{\sin(v-\tilde{\theta}_0-\mathrm{i}\gamma)}{\sin(v-\tilde{\theta}_0)} & \text{for} \quad \operatorname{Im}\tilde{\theta}_0+\gamma < \delta \\ \dfrac{\cos(v-\mathrm{i}\delta)}{\cos(v+\mathrm{i}\gamma-\mathrm{i}\delta)} & \text{for} \quad \delta < \operatorname{Im}\tilde{\theta}_0+\gamma \end{cases}$$

$$\varphi_0^{(1)}(v) = \frac{\sin(v-\theta_1+\mathrm{i}\gamma)\sin(v+\theta_1^*+\mathrm{i}\gamma)}{\sin(v-\theta_1)\sin(v+\theta_1^*)} \qquad \overline{\varphi}_0(v) = \overline{\varphi}_0^{(0)}(v)\overline{\varphi}_0^{(\bar{0})}(v)\overline{\varphi}_0^{(\tilde{0})}(v)\overline{\varphi}_0^{(1)}(v)$$

$$\varphi_0(v) = \varphi_0^{(0)}(v)\varphi_0^{(\tilde{0})}(v)\varphi_0^{(1)}(v) \qquad \varphi_1(v) = \varphi_0(v)\overline{\varphi}_0(v).$$

The additional term $\chi(v)$ in (3.8) is determined from

$$\chi(v) = \chi^{(0)}(v)\chi^{(\bar{0})}(v)\chi^{(\tilde{0})}(v)\chi^{(1)}(v)$$

$$\chi^{(0)}(v) = \begin{cases} 1 \quad \text{for} \quad \operatorname{Im}\theta_0 < -\delta \\ \dfrac{\sin(v-\theta_0+\frac{\mathrm{i}}{2}\gamma\alpha)\cos(v-\frac{\mathrm{i}}{2}\gamma(\alpha+2)+\mathrm{i}\delta)}{\sin(v-\theta_0-\frac{\mathrm{i}}{2}\gamma(\alpha+2))\cos(v+\frac{\mathrm{i}}{2}\gamma\alpha+\mathrm{i}\delta)} \\ \text{for} \quad -\delta < \operatorname{Im}\theta_0 < 0 \\ \dfrac{\sin(v-\theta_0-\frac{\mathrm{i}}{2}\gamma\alpha)\cos(v-\frac{\mathrm{i}}{2}\gamma(\alpha+2)+\mathrm{i}\delta)\cos(v+\frac{\mathrm{i}}{2}\gamma\alpha)\cos(v+\frac{\mathrm{i}}{2}\gamma(\alpha+2))}{\sin(v-\theta_0+\frac{\mathrm{i}}{2}\gamma(\alpha+2))\cos(v+\frac{\mathrm{i}}{2}\gamma\alpha+\mathrm{i}\delta)\cos(v-\frac{\mathrm{i}}{2}\gamma(\alpha+2))\cos(v-\frac{\mathrm{i}}{2}\gamma\alpha)} \\ \text{for} \quad 0 < \operatorname{Im}\theta_0 < \delta \\ \dfrac{\cos(v-\frac{\mathrm{i}}{2}\gamma\alpha-\mathrm{i}\delta)\cos(v-\frac{\mathrm{i}}{2}\gamma(\alpha+2)+\mathrm{i}\delta)\cos(v+\frac{\mathrm{i}}{2}\gamma\alpha)\cos(v+\frac{\mathrm{i}}{2}\gamma(\alpha+2))}{\cos(v+\frac{\mathrm{i}}{2}\gamma(\alpha+2)-\mathrm{i}\delta)\cos(v+\frac{\mathrm{i}}{2}\gamma\alpha+\mathrm{i}\delta)\cos(v-\frac{\mathrm{i}}{2}\gamma(\alpha+2))\cos(v-\frac{\mathrm{i}}{2}\gamma\alpha)} \\ \text{for} \quad \delta < \operatorname{Im}\theta_0 \end{cases}$$

$$\chi^{(\bar{0})}(v) = \begin{cases} 1 \qquad \text{for} \quad \operatorname{Im}\overline{\theta}_0 < -\delta \\ \dfrac{\sin(v-\overline{\theta}_0+\frac{\mathrm{i}}{2}\gamma\alpha)\cos(v-\frac{\mathrm{i}}{2}\gamma(\alpha+2)+\mathrm{i}\delta)}{\sin(v-\overline{\theta}_0-\frac{\mathrm{i}}{2}\gamma(\alpha+2))\cos(v+\frac{\mathrm{i}}{2}\gamma\alpha+\mathrm{i}\delta)} \\ \text{for} \quad -\delta < \operatorname{Im}\overline{\theta}_0 < 0 \end{cases} \tag{C.23}$$

$$\chi^{(\tilde{0})}(v) = \begin{cases} 1 \qquad \text{for} \quad 0 < \operatorname{Im}\tilde{\theta}_0+\gamma < \delta \\ \dfrac{\sin(v-\tilde{\theta}_0-\frac{\mathrm{i}}{2}\gamma(\alpha+2))\cos(v+\frac{\mathrm{i}}{2}\gamma(\alpha+2)-\mathrm{i}\delta)}{\sin(v-\tilde{\theta}_0+\frac{\mathrm{i}}{2}\gamma\alpha)\cos(v-\frac{\mathrm{i}}{2}\gamma\alpha-\mathrm{i}\delta)} \\ \text{for} \quad \operatorname{Im}\tilde{\theta}_0 < -\delta \quad \delta < \operatorname{Im}\tilde{\theta}_0+\gamma \\ \dfrac{\cos(v-\frac{\mathrm{i}}{2}\gamma(\alpha+2)+\mathrm{i}\delta)\cos(v+\frac{\mathrm{i}}{2}\gamma(\alpha+2)-\mathrm{i}\delta)}{\cos(v+\frac{\mathrm{i}}{2}\gamma\alpha+\mathrm{i}\delta)\cos(v-\frac{\mathrm{i}}{2}\gamma\alpha-\mathrm{i}\delta)} \\ \text{for} \quad -\delta < \operatorname{Im}\tilde{\theta}_0 < 0 \end{cases}$$

$$\chi^{(1)}(v) = \frac{\sin(v-\theta_1-\frac{\mathrm{i}}{2}\alpha\gamma)\sin(v+\theta_1^*-\frac{\mathrm{i}}{2}\alpha\gamma)}{\sin(v-\theta_1+\frac{\mathrm{i}}{2}\gamma(\alpha+2))\sin(v+\theta_1^*+\frac{\mathrm{i}}{2}\gamma(\alpha+2))} \times \begin{cases} 1 \qquad \text{for} \quad \operatorname{Im}\theta_1 < -\delta \\ \dfrac{\sin(v-\theta_1-\frac{\mathrm{i}}{2}\gamma(\alpha+2))\sin(v+\theta_1^*-\frac{\mathrm{i}}{2}\gamma(\alpha+2))\cos^2(v+\frac{\mathrm{i}}{2}\gamma\alpha+\mathrm{i}\delta)}{\sin(v-\theta_1+\frac{\mathrm{i}}{2}\alpha\gamma)\sin(v+\theta_1^*+\frac{\mathrm{i}}{2}\alpha\gamma)\cos^2(v-\frac{\mathrm{i}}{2}\gamma(\alpha+2)+\mathrm{i}\delta)} \\ \text{for} \quad -\delta < \operatorname{Im}\theta_1 < 0. \end{cases}$$

Appendix D. Analytic continuation for NLIE

The above-derived NLIEs are well defined only in the region $-\gamma+\delta < \operatorname{Im} v < 0$ for $\ln \mathfrak{a}_0(v)$, $0 < \operatorname{Im} v < \gamma-\delta$ for $\ln \overline{\mathfrak{a}}_0(v)$ and $-\delta < \operatorname{Im} v < \delta$ for $\ln \mathfrak{a}_1(v)$. To determine the integration constants (which should be determined from the limit $\mathrm{i}|v| \to \infty$) and the additional zeros for the excited states, we must extend the region by using the analytic continuation. We can achieve this by applying Cauchy's theorem to the convolutions. As a consequence, the additional terms appear due to the residues of the kernels. The resultant equations can be written explicitly as follows:

$$\begin{aligned} \ln \mathfrak{a}_0(v) &= \psi(v) + k_0 \overset{\overline{C}_0}{*} \ln \overline{\mathfrak{A}}_0(v) + k_0 \overset{C_1}{*} \ln \mathfrak{A}_1(v) + \beta\mu - \varphi_0^{\mathrm{c}}(v) \\ \ln \overline{\mathfrak{a}}_0(v) &= \psi(-v) + \overline{k}_0 \overset{C_0}{*} \ln \mathfrak{A}_0(v) + \overline{k}_0 \overset{C_1}{*} \ln \mathfrak{A}_1(v) + \beta\mu - \overline{\varphi}_0^{\mathrm{c}}(v) \\ \ln \mathfrak{a}_1(v) &= \psi(v) + \psi(-v) + \overline{k}_0 \overset{C_0}{*} \ln \mathfrak{A}_0(v) + k_0 \overset{\overline{C}_0}{*} \ln \overline{\mathfrak{A}}_0(v) \\ &\quad + k_1 \overset{C_1}{*} \ln \mathfrak{A}_1(v) + 2\beta\mu - \varphi_1^{\mathrm{c}}(v) \end{aligned} \tag{D.1}$$

where

$$\varphi_0^{\mathrm{c}}(v) = \begin{cases} \ln \overline{\mathfrak{A}}_0(v+\mathrm{i}\gamma) + \ln \mathfrak{A}_1(v+\mathrm{i}\gamma) & \text{for} \quad \operatorname{Im} v < -\gamma \\ \ln \overline{\mathfrak{A}}_0(v+\mathrm{i}\gamma) & \text{for} \quad -\gamma < \operatorname{Im} v < -\gamma+\delta \\ 0 & \text{for} \quad -\gamma+\delta < \operatorname{Im} v < 0 \\ \ln \mathfrak{A}_1(v) & \text{for} \quad 0 < \operatorname{Im} v < \delta \\ \ln \overline{\mathfrak{A}}_0(v) + \ln \mathfrak{A}_1(v) & \text{for} \quad \delta < \operatorname{Im} v \end{cases}$$

$$\overline{\varphi}_0^{\mathrm{c}}(v) = \begin{cases} \ln \mathfrak{A}_0(v) + \ln \mathfrak{A}_1(v) & \text{for} \quad \operatorname{Im} v < -\delta \\ \ln \mathfrak{A}_1(v) & \text{for} \quad -\delta < \operatorname{Im} v < 0 \\ 0 & \text{for} \quad 0 < \operatorname{Im} v < \gamma - \delta \\ \ln \mathfrak{A}_0(v - \mathrm{i}\gamma) & \text{for} \quad \gamma - \delta < \operatorname{Im} v < \gamma \\ \ln \mathfrak{A}_0(v - \mathrm{i}\gamma) + \ln \mathfrak{A}_1(v - \mathrm{i}\gamma) & \text{for} \quad \gamma < \operatorname{Im} v \end{cases} \tag{D.2}$$

$$\varphi_1^{\mathrm{c}}(v) = \begin{cases} \ln \mathfrak{A}_0(v) + \ln \overline{\mathfrak{A}}_0(v + \mathrm{i}\gamma) + \ln \mathfrak{A}_1(v + \mathrm{i}\gamma) & \text{for} \quad \operatorname{Im} v < -\gamma \\ \ln \mathfrak{A}_0(v) + \ln \overline{\mathfrak{A}}_0(v + \mathrm{i}\gamma) & \text{for} \quad -\gamma < \operatorname{Im} v < -\gamma + \delta \\ \ln \mathfrak{A}_0(v) & \text{for} \quad -\gamma + \delta < \operatorname{Im} v < -\delta \\ 0 & \text{for} \quad -\delta < \operatorname{Im} v < \delta \\ \ln \overline{\mathfrak{A}}_0(v) & \text{for} \quad \delta < \operatorname{Im} v < \gamma - \delta \\ \ln \overline{\mathfrak{A}}_0(v) + \ln \mathfrak{A}_0(v - \mathrm{i}\gamma) & \text{for} \quad \gamma - \delta < \operatorname{Im} v < \gamma \\ \ln \overline{\mathfrak{A}}_0(v) + \ln \mathfrak{A}_0(v - \mathrm{i}\gamma) + \ln \mathfrak{A}_1(v - \mathrm{i}\gamma) & \text{for} \quad \gamma < \operatorname{Im} v. \end{cases}$$

Similarly, the NLIE for the eigenvalue can be written as follows:

$$\ln \Lambda(v) = \Psi(v) + \zeta * \ln \mathfrak{A}_0(v) + \overline{\zeta} * \ln \overline{\mathfrak{A}}_0(v) + (\zeta + \overline{\zeta}) * \ln \mathfrak{A}_1(v) + \chi_0^{\mathrm{c}}(v) + \overline{\chi}_0^{\mathrm{c}}(v) + \chi_1^{\mathrm{c}}(v) \tag{D.3}$$

where

$$\chi_0^{\mathrm{c}}(v) = \begin{cases} \ln \mathfrak{A}_0\left(v + \dfrac{\mathrm{i}}{2}\gamma\alpha\right) & \text{for} \quad \operatorname{Im} v < -\frac{\gamma}{2}\alpha - \delta \\ 0 & \text{for} \quad -\frac{\gamma}{2}\alpha - \delta < \operatorname{Im} v < \frac{\gamma}{2}(\alpha + 2) - \delta \\ \ln \mathfrak{A}_0\left(v - \dfrac{\mathrm{i}}{2}\gamma(\alpha + 2)\right) & \text{for} \quad \frac{\gamma}{2}(\alpha + 2) - \delta < \operatorname{Im} v \end{cases}$$

$$\overline{\chi}_0^{\mathrm{c}}(v) = \begin{cases} \ln \overline{\mathfrak{A}}_0\left(v + \dfrac{\mathrm{i}}{2}\gamma(\alpha + 2)\right) & \text{for} \quad \operatorname{Im} v < -\frac{\gamma}{2}(\alpha + 2) + \delta \\ 0 & \text{for} \quad -\frac{\gamma}{2}(\alpha + 2) + \delta < \operatorname{Im} v < \frac{\gamma}{2}\alpha + \delta \\ \ln \overline{\mathfrak{A}}_0\left(v - \dfrac{\mathrm{i}}{2}\gamma\alpha\right) & \text{for} \quad \frac{\gamma}{2}\alpha + \delta < \operatorname{Im} v \end{cases} \tag{D.4}$$

$$\chi_1^{\mathrm{c}}(v) = \begin{cases} \ln \mathfrak{A}_1\left(v + \dfrac{\mathrm{i}}{2}\gamma\alpha\right) + \ln \mathfrak{A}_1\left(v + \dfrac{\mathrm{i}}{2}\gamma(\alpha + 2)\right) & \text{for} \quad \operatorname{Im} v < -\frac{\gamma}{2}(\alpha + 2) \\ \ln \mathfrak{A}_1\left(v + \dfrac{\mathrm{i}}{2}\gamma\alpha\right) & \text{for} \ -\frac{\gamma}{2}(\alpha + 2) < \operatorname{Im} v < -\frac{\gamma}{2}\alpha \\ 0 & \text{for} \quad -\frac{\gamma}{2}\alpha < \operatorname{Im} v < \frac{\gamma}{2}\alpha \\ \ln \mathfrak{A}_1\left(v - \dfrac{\mathrm{i}}{2}\gamma\alpha\right) & \text{for} \quad \frac{\gamma}{2}\alpha < \operatorname{Im} v < \frac{\gamma}{2}(\alpha + 2) \\ \ln \mathfrak{A}_1\left(v - \dfrac{\mathrm{i}}{2}\gamma\alpha\right) + \ln \mathfrak{A}_1\left(v - \dfrac{\mathrm{i}}{2}\gamma(\alpha + 2)\right) & \text{for} \quad \frac{\gamma}{2}(\alpha + 2) < \operatorname{Im} v. \end{cases}$$

References

[1] Korepin V E, Bogoliubov N M and Izergin A G 1993 *Quantum Inverse Scattering Method and Correlation Functions* (Cambridge: Cambridge University Press)

[2] Belavin A A, Polyakov A M and Zamolodchikov A B 1984 *Nucl. Phys.* B **241** 333

[3] Cardy J L 1986 *Nucl. Phys.* B **270** 186

[4] Kawakami N and Yang S-K 1990 *Phys. Lett.* A **148** 359

[5] Frahm H and Korepin V E 1990 *Phys. Rev.* B **42** 10553

[6] Suzuki M 1985 *Phys. Rev.* B **31** 2957
[7] Suzuki M and Inoue M 1987 *Prog. Theor. Phys.* **78** 787
[8] Inoue M and Suzuki M 1988 *Prog. Theor. Phys.* **79** 645
[9] Koma T 1987 *Prog. Theor. Phys.* **78** 1213
[10] Suzuki J, Akutsu Y and Wadati M 1990 *J. Phys. Soc. Japan* **59** 2667
[11] Suzuki J, Nagao T and Wadati M 1992 *Int. J. Mod. Phys.* B **6** 1119–80
[12] Destri C and de Vega H J 1992 *Phys. Rev. Lett.* **69** 2313
[13] Takahashi M 1991 *Phys. Rev.* B **43** 5788
[14] Mizuta H, Nagao T and Wadati M 1994 *J. Phys. Soc. Japan* **63** 3951
[15] Klümper A 1992 *Ann. Phys., Lpz.* **1** 540
[16] Klümper A 1993 *Z. Phys.* B **91** 507
[17] Yang C N and Yang C P 1969 *J. Math. Phys.* **10** 1115
[18] Gaudin M 1971 *Phys. Rev. Lett.* **26** 1301
[19] Takahashi M 1971 *Prog. Theor. Phys.* **46** 401
[20] Kuniba A, Sakai K and Suzuki J 1998 *Nucl. Phys.* B **525** 597
[21] Sakai K, Shiroishi M, Suzuki J and Umeno Y 1999 *Phys. Rev.* B **60** 5186
[22] Sakai K 1999 *J. Phys. Soc. Japan* **68** 1789
[23] Klümper A, Martínez J R R, Scheeren C and Shiroishi M 2001 *J. Stat. Phys.* **102** 937
(Klümper A, Martínez J R R, Scheeren C and Shiroishi M 2000 *Preprint* cond-mat/0004379)
[24] Bariev R Z, Klümper A and Zittartz J 1995 *Europhys. Lett.* **32** 85
[25] Kulish P P and Sklyanin E K 1982 *J. Sov. Math.* **19** 1596
[26] Gould M D, Hibberd K E, Links J R and Zhang Y-Z 1996 *Phys. Lett.* A **212** 156
[27] Bracken A J, Gould M D, Links J R and Zhang Y-Z 1995 *Phys. Rev. Lett.* **74** 2768
[28] Ramos P B and Martins M J 1996 *Nucl. Phys.* B **474** 678
[29] Pfannmüller M P and Frahm H 1996 *Nucl. Phys.* B **479** 575
[30] Bedürftig G and Frahm H 1995 *J. Phys. A: Math. Gen.* **28** 4453
[31] Jüttener G, Klümper A and Suzuki J 1997 *J. Phys. A: Math. Gen.* **30** 1881
[32] Klümper G, Batchelor M T and Pearce P A 1991 *J. Phys. A: Math. Gen.* **24** 3111
[33] Eßler F H L, Korepin V E and Schoutens K 1992 *Phys. Rev. Lett.* **68** 2960
[34] Eßler F H L, Korepin V E and Schoutens K 1993 *Phys. Rev. Lett.* **70** 73
[35] Alcaraz F C and Bariev R Z 1999 *J. Phys. A: Math. Gen.* **32** 483
[36] Ramos P B and Martins M J 1997 *J. Phys. A: Math. Gen.* **30** L195